

63-33

403304

ASD-TDR-63-296

CATALOGED BY ASTIA
FILED

VACUUM ARC MELTING OF TUNGSTEN +0.6 COLUMBIUM

TECHNICAL DOCUMENTARY REPORT NO. ASD-TDR-63-296
April 1963

Directorate of Materials and Processes
Aeronautical Systems Division
Air Force Systems Command
Wright-Patterson Air Force Base, Ohio

Project No. 7351, Task No. 735104

ASTIA
RECEIVED
MAY 1 1963
ASTIA

(Prepared under Contract No. AF 33(616)-7459 by
the Westinghouse Electric Corp., Blairsville, Pa.,
George A. Reimann, author.)

NOTICES

When Government drawings, specifications, or other data are used for any purpose other than in connection with a definitely related Government procurement operation, the United States Government thereby incurs no responsibility nor any obligation whatsoever; and the fact that the Government may have formulated, furnished, or in any way supplied the said drawings, specifications, or other data, is not to be regarded by implication or otherwise as in any manner licensing the holder or any other person or corporation, or conveying any rights or permission to manufacture, use, or sell any patented invention that may in any way be related thereto.

Qualified requesters may obtain copies of this report from the Armed Services Technical Information Agency, (ASTIA), Arlington Hall Station, Arlington 12, Virginia.

This report has been released to the Office of Technical Services, U.S. Department of Commerce, Washington 25, D.C., for sale to the general public.

Copies of this report should not be returned to the Aeronautical Systems Division unless return is required by security considerations, contractual obligations, or notice on a specific document.

FOREWORD

This report was prepared by Westinghouse Electric Corporation under USAF Contract No. 33(616)-7459. This contract was initiated under Project Number 7351, Task Number 735101. The work was administered under the direction of the Directorate of Materials and Processes, Aeronautical Systems Division, with Mr. Shingo Inouye as Air Force Project Engineer.

The program was conducted under the technical direction of George A. Reimann, Project Engineer. Significant contributions have been made to the program by Messrs. Shingo Inouye and George Saul, ASD, and by Messrs. A. W. Goldstein and R. A. Sweeney of Westinghouse.

This report covers the work done from 1 August, 1962 to 28 February, 1963.

ABSTRACT

Vacuum arc melting techniques were developed to produce sound 3½-inch and 4-inch diameter ingots of tungsten base alloys. The effect of melting rate on ingot characteristics was determined and the effects of carbon, oxygen, zirconium and titanium on melting characteristics, ingot structure, extrudability, recrystallization, and high temperature tensile properties of the W+0.6%Cb alloy were studied also.

Refinement of ingot structure was produced by 0.06 and 0.12% zirconium additions and by increasing the melting rate. Coarsening of ingot structure was produced by 0.04% titanium and 500 to 1000 ppm oxygen additions.

W+0.6Cb ingots containing more than 50 ppm carbon could not be extruded, and correlation between extrudability vs. carbon content below 50 ppm was not found.

Adding 0.12% zirconium to the W+0.6Cb alloy significantly improved the 3000°F tensile properties.

PUBLICATION REVIEW

This technical documentary report has been reviewed and is approved.

FOR THE COMMANDER:



I. PERLMUTTER
Chief, Physical Metallurgy Branch
Metals and Ceramics Laboratory
Directorate of Materials & Processes

TABLE OF CONTENTS

	<u>Page</u>
I. INTRODUCTION	1
II. PROGRAM	2
III. PROCEDURE AND RESULTS, PHASE I	3
A. Electrodes	
B. Melting	
IV. PROCEDURE AND RESULTS, PHASE II	6
A. Electrodes	
B. Melting	
V. PROCEDURE AND RESULTS, PHASE III	10
VI. MICROSTRUCTURES AND INGOT CHEMISTRY	13
VII. PRIMARY BREAKDOWN AND SUBSEQUENT EVALUATION	17
A. Extrusion	
B. Forging	
C. Recrystallization	
D. Swaging	
E. Tensile Testing	
VIII. INTERNAL SUPPORT	26
IX. EQUIPMENT MODIFICATIONS	27
X. CONCLUSIONS	28
XI. REFERENCES	29

LIST OF TABLES

<u>Table</u>	<u>Title</u>	<u>Page</u>
1	Electrode Characteristics	30
2	Suppliers' Analyses of Melting Material	31
3	Individual Electrode Analyses	32
4	Typical Melt Record of W+0.6Cb	33
5	Summary of W+0.6Cb Arc Melting Data	34
6	W+0.6Cb Ingot Analyses	35
7	Relative Interstitial Level of Electrodes, Electrode Stubs, and Ingots	36
8	Comparative Carbon and Oxygen Analyses for W+0.6Cb Samples	37
9	Hardness of W+0.6Cb Ingots	38
10	Summary of W+0.6Cb Extrusion Data	39
11	Hardness of W+0.6Cb Extrusions	40
12	Tensile Data on Swaged W+0.6Cb Alloy	41
13	Summary of Vacuum Arc Melting for Support Program	42

LIST OF FIGURES

<u>Figure</u>	<u>Title</u>	<u>Page</u>
1	Vacuum Arc Melting Facility at ASD	43
2	Redesigned Water Jacket Assembly Mounted on Furnace	44
3	Examples of Threaded Electrode Sections . . .	45
4	Ingot Sections of W+0.6Cb Heats VA-66 and VA-67	46
5	Method of Cutting W+0.6Cb Ingots for Samples and Billet	47
6	W+0.6Cb Ingot VA-83	48
7	Macrostructures of W+0.6Cb Ingots VA-83, VA-87, VA-88 and VA-91	49
8	Macrostructures of W+0.6Cb Ingots VA-86, VA-90, and VA-92	50
9	Macrostructures of W+0.6Cb Ingots VA-78, VA-79, and VA-80	51
10	Melting Rate vs. Input for W+0.6Cb Alloy . . .	52
11	Macrostructures of W+0.6Cb Ingots VA-81, VA-85, VA-82, and VA-89	53
12	Microstructures of W+0.6Cb Ingots VA-66 and VA-67	54
13	Microstructures of W+0.6Cb Ingots VA-83 and VA-87	55
14	Microstructures of W+0.6Cb Ingots VA-88 and VA-91	56
15	Microstructures of W+0.6Cb Ingots VA-86 and VA-92	57
16	Microstructures of W+0.6Cb Ingots VA-78, VA-79, and VA-80	58

LIST OF FIGURES
(continued)

<u>Figure</u>	<u>Title</u>	<u>Page</u>
17	Microstructures of W+0.6Cb Ingots VA-81 and VA-85	59
18	Microstructures of W+0.6Cb Ingots VA-82 and VA-89	60
19	Electrode Stubs before Removal of Chemistry Samples	61
20	Machined Billet and Unextruded Billet from Ingot VA-83 (High Carbon) and Machined Billet from VA-90 (High Oxygen)	62
21	Extrusions of W+0.6Cb Alloy	63
22	Intergranular Deposit in Unextruded Billet from Ingot VA-68	64
23	Closeup of Extrusion Surfaces	65
24	Closeup of Extrusion Surfaces Showing Defects Peculiar to Material Originating from High Oxygen Electrodes	66
25	Extrusion Sample Identification Diagram	67
26	Transverse and Longitudinal Macrosections of Extrusions 956 and 974	68
27	Microstructures from Nose, Center, and Tail Samples of Extrusions 935 and 936	69
28	Microstructures from Nose, Center, and Tail Samples of Extrusions 946 and 947	70
29	Microstructures from Nose, Center, and Tail Samples of Extrusions 955 and 956	71
30	Microstructures from Nose, Center, and Tail Samples of Extrusions 964 and 965	72
31	Microstructures from Nose, Center, and Tail Samples of Extrusion 974	73

LIST OF FIGURES
(continued)

<u>Figure</u>	<u>Title</u>	<u>Page</u>
32	Extrusion Forging Samples, Machined Forging Samples, and Forged Samples of W+0.6Cb Alloy .	74
33	l/T vs. Time for Recrystallization of W+0.6Cb	75
34	Effect of Recrystallization Heat Treatment on W+0.6Cb Extrusion Samples that were Annealed and Reduced 55% by Forging	76
35	Microstructures of W+0.6Cb Extrusion Samples Reduced 40% by Swaging	77
36	Microstructures of W+0.6Cb Extrusion Samples Reduced 40% by Swaging, Annealed, Reduced Additional 56% by Swaging	78
37	Standard Refractory Alloy Vacuum Creep-Rupture Specimen	79
38	Threaded Electrode Sections of 94% Tungsten - 6% Molybdenum	80
39	Ingots of 92-6-2 Alloy Containing Surface Defects	81
40	Melting Rate vs. Input for 92-6-2 Alloy . . .	82
41	Ingots of Pure Columbium (VA-77) Produced in 2-Inch Mold	83
42	Comparison of 3½-Inch and 2-Inch Molds and Accessories	84

I. INTRODUCTION

Tungsten and certain tungsten base alloys possess some of the best high temperature properties obtainable, but lack of satisfactory processing techniques has prevented utilization of this element to its full potential. The characteristics of the tungsten arc, coupled with the metal's extreme melting point, are among many of the problems of arc melting. Lack of ingot fabricability is often related to arc melting practice.

The successful generation of tungsten ingots has become rather commonplace using arc melting techniques, but subsequent fabricability often remains a problem. Even at very low concentrations, certain impurities are believed to have a significant effect on fabricability. It is difficult to relate a specific effect to a specific impurity. Very few reliable procedures have been developed to determine minor concentrations, or to identify and correlate the effect of impurity distributions. The development of analyses to detect such minute quantities was beyond the scope of this program, however, much of the success of this investigation depended to a large extent on the sophistication of certain analytical techniques that were necessary for meaningful metallurgical studies.

It is generally believed that lack of tungsten fabricability is primarily a grain boundary effect, even at somewhat elevated temperatures. Arc melting should not be considered as a cause of this effect, but rather as a step in the process where it is advantageous to remove deleterious impurities and produce a structure that lends itself more readily to plastic deformation.

The objectives of this program were to establish a consistent melting technique for the production of sound, homogeneous, tungsten alloy ingots which could be converted into 3-inch diameter extrusion billets approximately 5-inches long with a minimum of machining. The effect of melting variables and minor alloying additions on tungsten alloy ingot characteristics and subsequent workability was studied also. The program was a continuation of USAF Contract No. AF 33(616)-7459, under which the Equipment Investigation and Development Program (Ref. ASD-TR-61-385) and the Tungsten-Molybdenum-Columbium Alloy Melting Program (Ref. ASD-TDR-62-781) were conducted. During these programs, the furnace shown in Figure 1 was designed and built to melt refractory alloys under high vacuum, a reproducible process was developed to produce Mo-0.5Ti billets with a refined grain structure, and a process was developed to produce sound billets of 92W-6Mo-2Cb alloy.

Manuscript released by the author April 1963 for publication as an ASD Technical Documentary Report.

II. PROGRAM

The experimental work for this program was organized into three phases, as follows:

A. Phase I

Four ingots were scheduled to develop a basic arc melting practice for the tungsten+0.6% columbium alloy.

B. Phase II

Seven ingots were scheduled to determine the effect of electrode carbon level and electrode oxygen level on arc melting characteristics and ingot fabricability. Three levels of carbon and three levels of oxygen were used for this study.

C. Phase III

Six ingots were scheduled to determine the effect of melting rate and minor additions of zirconium and titanium on arc melting characteristics and ingot fabricability. Two ingots were used for the melting rate study and four ingots were used to evaluate alloying additions.

The following sections of text, containing the discussion of procedure and the results of work performed during the contractual period, are organized in a manner similar to that just given under "Program". Ingots were melted as appropriate electrode material became available and not in a numerical sequence related to their order of description under "Program". The following summary is presented to show the relation of ingot number to program phases.

Phase I

<u>Ingot</u>	<u>Amperage</u>	<u>Additions</u>	<u>Disposition</u>
VA-66	4800	---	Sectioned for macro
VA-67	5400	---	Sectioned for macro
VA-68	5500	---	Did not extrude
VA-78	5800	---	Extruded and evaluated

Phase II

VA-83	6000	150ppm C	Did not extrude
VA-86	5800	50ppm O	Extruded and evaluated
VA-87	5800	100ppm C	Did not extrude
VA-88	5800	250ppm C	Did not extrude
VA-90	5800	100ppm O	Extruded and evaluated

Phase II
(continued)

<u>Ingot</u>	<u>Amperage</u>	<u>Additions</u>	<u>Disposition</u>
VA-91	6000	250ppm C + 990ppm Ti	Did not extrude
VA-92	5800	150ppm O	Extruded and evaluated

Interstitial additions were "specified" analysis.

Phase III

VA-79	6500	---	Extruded and evaluated
VA-80	7200	---	Sectioned for macro
VA-81	6200	.06% Zr	Extruded and evaluated
VA-82	6000	.04% Ti	Extruded and evaluated
VA-85	6000	.12% Zr	Extruded and evaluated
VA-89	6000	.12% Zr + .04% Ti	Extruded and evaluated

III. PROCEDURE AND RESULTS, PHASE I

A. Electrodes

A high purity tungsten starting material is required to minimize effects of residual elements on arc melting characteristics and subsequent material fabricability, even though the vacuum arc melting step itself is quite effective in reducing the level of residual elements. Certain levels of oxygen, carbon, iron and silicon were believed to have adverse effects on fabricability, however a number of other elements are present in minor amounts and the influence of many of these has not been clearly established, nor have effective analytical procedures been developed to determine quantities of some elements which are present at very low concentrations.

No facilities exist at ASD to produce pressed and sintered electrodes, and although such a facility could not significantly increase the purity of the material received, it would enable closer correlation of electrode fabrication variables with arc melting conditions and arc cast material fabricability. This program relied upon outside suppliers for the majority of the electrode material used and depended upon their experience, quality control, and process reproducibility to insure that a uniform material of high purity was obtained. Generally, specific details on a commercially successful process are considered proprietary.

All of the electrodes used for Phases I and III were manufactured by the General Electric Corporation. This material was ordered as high purity tungsten powder, hydrostatically pressed and hydrogen sintered to a minimum of 88 percent of theoretical density. Specified bar dimensions were 1½" O.D. x ¼" I.D. x 24" length. Table 1 lists the characteristics of the material received.

An electrode diameter of 1½ inches was specified because two attempts to melt 1½-inch electrodes of the W+0.6Cb composition into 3½-inch diameter molds in the previous program⁽¹⁾ ended in crucible burn-through before the melting current could be increased to a level which would produce a satisfactory melting rate. No difficulties were encountered when 1½-inch electrodes of the 92W-6Mo-2Cb alloy were used, so the 1½-inch diameter was selected for this program. Notice in Table 1, however, that many of the electrode sections furnished for the program measured approximately 1¼-inches in diameter and, contrary to earlier experience, melted satisfactorily. This was attributed to more effective mold cooling resulting from improved mold and water jacket design, and to the installation of a water conditioner to the cooling water line.

Straightness and length specifications were difficult to meet in the 1½-inch diameter section and four of the first six bars received were returned to the supplier, mainly because of failure to meet the straightness requirement. Subsequent shipments were satisfactory in all respects.

All electrode sections were joined mechanically, and the 1-8NC thread was found to be most practical. The 1¼-7NC internal thread left insufficient sidewall and the ¼-10NC thread would not accommodate a boring bar of sufficient rigidity for satisfactory machining. Examples of threaded electrodes are shown in Figure 3.

Three diameters of columbium wire were purchased from R & D Metals Corp., Kidron, Ohio, for insertion into the ¼-inch electrodes bores. Early ingot analysis indicated that an 0.65 to 0.70 percent columbium addition in the electrode would produce 0.55 to 0.60 percent columbium in the ingot. Various combinations of 63, 91, and 125 mil columbium wire allowed latitude in electrode composition. The ends of the wire were bent over at the top of the electrode to prevent their sliding downward during melting. This is shown in Figure 3. The suppliers' analyses of columbium wire and tungsten electrodes are shown in Table 2.

B. Melting

The furnace installation shown in Figure 1 was employed for all melting during this program. It was designed for consumably melting refractory alloy electrodes into ingots up to 6 inches in diameter (with the water jacket shown in the photograph) using up to 7500 amperes direct current. All melting has been done with straight polarity (electrode negative). The two-stage mechanical pump and the large diffusion pump can maintain a vacuum of 0.05 to 0.1 microns in the furnace chamber during melting of tungsten alloy electrodes. Ingots for this program were produced in 3½-inch water cooled copper molds using the jacket assembly shown in Figure 2, both of which are described in detail in a previous report(1).

Four ingots were required for parametral study to enable completion of Phase I. As previously explained (see "Electrodes"), it was believed that an electrode diameter of 1¼ inches could not be melted satisfactorily into a 3½-inch mold. The first W+0.6Cb ingot was made to study the effect of electrode diameter and to verify that the 1¼-inch section was suitable for this program. Electrode O9115-2 was machined to provide three stepped sections of approximately equal length, one of the original 1¼-inch diameter; one of the 1½-inch diameter; and one of the 1¾-inch diameter. Both the 1¼ and the 1½-inch sections of this electrode were melted without difficulty using 4800 amperes and 28 volts. The longitudinal section of this ingot is shown in Figure 4. Three amperes stirring current were used for the entire heat, including hottopping, where it may be noted that this degree of stirring produced a high rim on the ingot. This heat was used to establish preliminary melting parameters only, and no chemistry samples were obtained because of the previous exposure of this electrode to the environment created by two mold failures.

The second ingot (VA-67) was melted from electrode O6208-6, which weighed 32 pounds. It was melted with 5400 amperes and 28 volts, with an average furnace pressure of 0.08 microns. The stirring current was reduced from 2 to 1 ampere during hottopping, but a fairly high rim is still present. The longitudinal section of this ingot is shown in Figure 4, and analytical results are listed in Table 6.

Ingot VA-68 was melted from electrode O6208-2 under essentially the same conditions as VA-67, except that 0.5 ampere stirring was used for most of the heat, greatly reducing the height of the rim. This ingot was too short to be sectioned

according to the desired procedure and still yield sufficient material for an extrusion billet. A shrinkage void was discovered in the ingot top during machining, and an additional .375-inch was machined from the billet length. The finish-machined billet measured 3.63 inches long and weighed only 16.9 pounds. Analytical results are shown in Table 6 and subsequent processing is discussed under "Primary Breakdown and Subsequent Evaluation".

Ingot VA-78 completed Phase I. It was melted with 5800 amperes, 28 volts and 3 amperes stirring. Furnace pressure averaged 0.03 microns during melting. Two electrode sections (G. E. 09297 series) were used to produce the desired 43 pounds which enabled the ingot to be sectioned according to the plan shown in Figure 9 and an entire longitudinal section would be expected to resemble ingot VA-67 (Figure 4) rather closely. Melting parameters used for this ingot are considered optimum for the equipment, electrode, and mold combination used. The "standard" melt record for producing W+0.6Cb ingots is shown as Table 4. Other melting details for this ingot are shown in Table 5 and analytical results are shown in Table 6.

IV. PROCEDURE AND RESULTS, PHASE II

Phase II involved a limited study of the effects of several electrode carbon and oxygen levels on the arc melting characteristics, ingot structure, and workability of the W+0.6Cb alloy. A comparison of ingot analysis and electrode analysis was made to determine the carbon and oxygen lost during melting, microexamination disclosed the effect of carbon and oxygen on structure, and extrusion determined the effect of carbon and oxygen on workability. Results were compared to data from ingots generated during Phases I and III that were made from electrodes containing minimum carbon and oxygen, and to applicable data obtained by other investigators.

A. Electrodes

Suppliers were reluctant to quote on electrode material containing oxygen greater than 100 ppm or containing both oxygen and carbon at specified levels. Also, suppliers of vacuum sintered material had difficulty meeting the straightness requirement of 1/16-inch maximum bow (camber) per foot. This is evident upon examination of the "camber" column in Table 1.

General Electric supplied the 09115 and the 11234 series electrodes. The 09115 material was reported to

contain 135 ppm carbon, 12 ppm oxygen, and the 11234 material was reported to contain 240 ppm carbon and 4 ppm oxygen. General Electric's manufacturing process involves a hydrogen sintering cycle that makes it difficult to retain appreciable amounts of oxygen.

Wah Chang supplied five vacuum sintered electrodes which are listed as the "WC" series in Table 1. After hydrostatic pressing at 40,000 psi these bars were subject to vacuum sintering at 1800°C (3270°F) for two hours, and to hydrogen sintering at 2200°C (4000°F) for five hours. Supplier's samples were reported to contain less than 30 ppm carbon and 50 to 60 ppm oxygen. Wah Chang's process permitted blending 0.70 percent columbium powder with tungsten prior to sintering, eliminating the requirement of hollow electrodes for wire additions.

Eight electrode sections were supplied by the Westinghouse Materials Manufacturing Division. The process developed there to produce these electrodes was similar to that employed by Wah Chang and involved blending of columbium with pure tungsten powder. Carbon was added as tungsten carbide and oxygen was added as Cb_2O_5 . The oxides of tungsten are easily reduced by heating in hydrogen and/or are too volatile when heated in vacuum to insure adequate retention of oxygen in the sintered product. The compacts were presintered in dry oxygen for two hours at 1250°C (2280°F). Densification occurs more rapidly in a hydrogen atmosphere and the comparatively low temperature was chosen to minimize carbon and oxygen losses. The hydrogen was evacuated from the chamber and the electrodes were sintered in vacuum for 5 hours at 1950°C (3540°F). Cooling to room temperature was done in vacuum to preclude the formation of columbium hydride. Bar analyses showed that columbium tended to concentrate in the lower end of the electrodes (which were sintered vertically), particularly in low carbon material. Insufficient data are available to indicate whether this condition was caused by insufficient blending, or had occurred during bag loading prior to pressing, or took place during the sintering process. The individual electrode analyses in Table 3 show the columbium to be well within specified limits, however the oxygen content was abnormally high. This condition did not prevent melting of ingots with a low oxygen content which could be extruded successfully.

B. Melting

Seven W+0.6Cb ingots were produced in Phase II. Four ingots (VA-83, 87, 88, 91) were melted from electrodes containing 100 ppm or more of carbon, and three ingots (VA-86, 90, 92) were melted from electrodes containing between 50 and 1000 ppm oxygen. Melting results are discussed in the following text, and additional evaluation is discussed under "Microstructures and Ingot Chemistry" and "Primary Breakdown and Subsequent Evaluation".

Two 1½-inch electrode sections, reported to contain 135 ppm carbon, were available for Phase II. In order not to risk mold failure, and to maintain essentially the same electrode-to-mold diameter ratio for all melting, these sections were machined to a 1.63-inch diameter. They averaged 34.5 pounds each and would produce rather short ingots if melted separately, so they were combined to make a single long ingot. VA-83 measured 14 inches long and weighed 80.1 pounds before removal of the hot top rim and starting pad. Melting details are summarized in Table 5. The ingot was cut into two 5-inch lengths, designated VA-83U (upper) and VA-83L (lower), and machined into two extrusion billets (Figure 20). The sample slice was cut from the center, between the two billet sections, instead of from the top as indicated by the sampling plan shown in Figure 5. The macrostructure of VA-83 and other ingots melted from high carbon electrodes is shown in Figure 7.

The remaining ingots made from high carbon electrodes were melted in a manner similar to that employed for VA-83. Furnace chamber pressure averaged somewhat higher for this material than for the high purity material. Also, the electrode consumption rate was somewhat greater (Figure 10), with the exception of VA-91 which contained a titanium addition. All ingot surfaces were rated very good to excellent and were very similar in appearance to VA-83 shown in Figure 6. Ingots were sampled according to the plan in Figure 5 (except VA-83) and the macrostructures are shown in Figure 7. All sections display a very fine, columnar as-cast grain size, which is generally considered desirable from the standpoint of fabricability. None of the ingots produced from high carbon electrodes could be extruded, however.

Ingot VA-91 deserves special mention. In view of the ability of titanium to "getter" unwanted impurities, and considering the reduced extrusion pressures required to generate extrusions from ingots produced from titanium-bearing electrodes in Phase III, two 11234 electrodes were used for study

to determine the ability of titanium to remove carbon from solution in tungsten. Available thermodynamic data⁽²⁾ indicated that titanium had considerably more affinity for carbon than did tungsten. Since the electrode material was reported to contain 240 ppm carbon, the approximate stoichiometric addition of titanium (990 ppm) was added in the form of 30-mil wire. The melting rate for this electrode was extremely slow, however the grain size remained fine in contrast to other ingots produced with slow melting rates or with titanium. It has not been ascertained how much of the carbon is in the form of titanium carbide, but the volume of grain boundary precipitate has increased noticeably (Figure 14). While the addition of titanium may have affected the composition of the carbide phase, it did little to change its distribution. The melting point of titanium carbide is somewhat lower than that of tungsten which would account for its presence on the grain boundaries. The billet produced from ingot VA-91 would not extrude.

The three ingots produced from electrodes containing a high oxygen content completed Phase II. The electrode material was produced by Wah Chang and by Westinghouse, using a vacuum sintering cycle. Columbium was added by blending it with tungsten powder prior to compaction. The first ingot of this series was VA-86, melted from a Wah Chang electrode. The consumption rate was high (Figure 10), considering the 5800 amperes melting current, and the furnace chamber pressure was low in comparison with pressures noted while melting other electrodes in the "high purity" category. This suggests that even with the 50-60 ppm reported oxygen content (and carbon), the Wah Chang electrodes were well suited to the arc melting process. Part of the high consumption rate was attributed to electrode fragmentation, which occurred continuously in the region of melting. The macrostructure for heat VA-86 is shown in Figure 8. The structure is fairly fine-grained, which is expected in view of a more rapid rate of ingot solidification.

Ingots VA-90 and VA-92 were made from Westinghouse electrodes. High oxygen contents were achieved by adding columbium as Cb_2O_5 . The effect of adding oxygen in this manner, as compared to having it present as one or more of the oxides of tungsten was not determined, and equilibrium data on oxygen distribution in liquid tungsten-columbium were not available. Furnace chamber pressures were considerably above average while melting these electrodes, ranging between 0.06 to 0.10 microns instead of the 0.03 to 0.04 microns which is considered normal. This suggests electrode out-gassing as a result of strong heating from resistance to the passage of 5800 amperes melting current, and/or that

a gas-producing reaction was taking place in the molten region. The electrode consumption rate was quite slow, and Figure 8 shows an extremely large as-cast grain size, similar to that found in electron beam melted ingots. Analytical data in Table 6 do not indicate that the difference in grain size between ingots VA-86, 90 and 92 is a result of compositional variation. In this instance at least, the electrode consumption rate, or more directly, the ingot solidification rate, was the sole factor influencing grain size.

The electrodes used for ingots VA-90 and VA-92 melted somewhat irregularly, and considerable sputtering and splashing occurred around the bath. The electrodes increased in diameter slightly near the region of melting as a result of an accumulation of frozen metal droplets ejected from the pool. Irregular electrode consumption produced ingot surfaces that were not as good as the average.

Based on the results of melting, and subsequent material evaluation performed on the ingots produced during Phase II, it appears that carbon was an undesirable addition in the quantities used, much more so than oxygen. Insufficient data are available from this investigation for an estimation of maximum carbon content permitting primary ingot breakdown by extrusion. It had occurred that oxygen additions could be used to control ingot carbon content in a similar manner as carbon additions are used to deoxidize arc cast molybdenum ingots. However, the data in Tables 7 and 8 indicate that carbon levels in W+0.6Cb are essentially unaffected by electrode oxygen content.

V. PROCEDURE AND RESULTS, PHASE III

The primary objectives of Phase III were to determine the effect of melting rate and alloying additions on the arc melting characteristics, ingot structure, chemistry, fabricability, and high temperature strength of the W+0.6Cb alloy. Results were compared to those generated in other phases of this program and to applicable data obtained by other investigators.

Two ingots were made using high melting currents and four ingots were made from electrodes containing relatively small amounts of zirconium and titanium to supplement the normal columbium addition. Ingots VA-79, 80, 82, 85 and 89 were melted from GE 09297 series electrodes. This electrode material has been described as part of Phase I.

Ingot VA-78, already described under Phase I, was used as the base line ingot for the melting rate study. The macrostructure is shown in Figure 9.

Ingot VA-79 was made using 6500 amperes and 28 volts, with 2.5 amperes stirring current. Furnace pressure averaged 0.04 microns. No difficulty was experienced as a result of exceeding the "standard" melting current by 500 to 700 amperes, although the cooling water began to boil occasionally near the end of the heat. The macro slice shows that increased melting current produces a finer grained structure (Figure 9) although this may have been achieved at the expense of a higher impurity content.

Since ingot VA-79 was completed successfully using 6500 amperes and there seemed to be some margin available for the use of additional current, 7200 amperes was used to melt VA-80. This approached the output capacity of the rectifiers. The electrode melted quite rapidly, as expected, but some consumption occurred as a result of electrode disintegration near the tip. Solid pieces of electrode were observed falling into the bath, but since this region was heated nearly to the melting point, no pieces of unmelted material were expected in the ingot.

Only four inches of electrode remained to be consumed when the cooling water began to boil violently and the current was shut off. This was the first instance since the new mold and jacket assembly were installed that a mold failure threatened, and although the mold was damaged somewhat, the current was turned off before penetration occurred. Some copper flowed down between the ingot and mold wall and provided a path for rapid heat transfer from the ingot. Cracking of the ingot resulted from thermal shock. The mold was cleaned and the damage was found to be slight. Five additional ingots were produced using this mold and it is still serviceable.

The transverse macrostructure of VA-80 is finer than that of VA-79, and it may be observed in Figure 9 that increases in melting current and the resulting increases in melting rate cause proportional refinements in grain structure. Melting rate, as influenced by power input, is shown in Figure 10, and electrode consumption data for other electrodes are shown also for comparison.

Ingot VA-80 was cut longitudinally in order to compare the entire ingot section to that of VA-67, which was melted at 5400 amperes. Again, the effect of electrode consumption rate, as influenced by power input, on ingot macrostructure was quite evident. In Phase II it was likewise demonstrated

that the ingot grain size varied with electrode consumption rate (Figures 8 and 10). In this case, power input was nearly constant and the consumption rate was apparently determined by the rate of oxygen elimination from the region of melting. Observe in Table 8 that the ingot oxygen content is essentially independent of electrode oxygen content.

No data could be found regarding the effect of minor additions of zirconium and titanium on the properties of the W+0.6Cb alloy, and only limited data were available on the effects of these additions on other tungsten-base systems. It was found in another investigation⁽³⁾ that the elevated temperature properties of unalloyed tungsten were improved by the addition of zirconium, titanium, and columbium, with columbium producing the most significant improvement. It was anticipated that minor amounts of zirconium and titanium would add to any property improvements already obtained by the presence of 0.6%Cb. Such a composition could be classified as a "TZW" alloy, similar to the abbreviations "TZM" and "TZC" currently applied to the molybdenum-base counterparts.

The electrode for ingot VA-81 contained a single 63-mil zirconium wire in addition to the normal amount of columbium, which added 0.06 percent zirconium per unit weight of melting stock. Previous experience with the 92W-6Mo-2Cb alloy⁽¹⁾ had shown that 0.25 percent zirconium in the electrode yielded 0.16 percent in the ingot, but this small addition rendered the 92-6-2 alloy unextrudable.

The electrode for VA-81 melted somewhat more slowly than normal (Figure 10) at 6200 amperes, and the furnace pressure averaged 0.04 microns. The macrostructure in Figure 11 exhibits a finer grain size than obtained previously under similar conditions of melting without the zirconium addition. Inasmuch as the factor limiting the amount of zirconium added to the electrode was the extrudability of the ingot, as determined in the previous program, it was apparent that the W+0.6Cb alloy would tolerate additional zirconium based on the extrudability of ingot VA-81 (Table 10). Ingot VA-85 was melted from an electrode containing 0.12 percent zirconium. The consumption rate was slightly greater than for VA-81 even with a lower melting current. The as-cast microstructure confirmed that zirconium is a grain refiner, as Figure 11 shows that additional zirconium produced an additional decrease in grain size.

Titanium wire was added to the electrode for heat VA-82 which produced a 0.04 percent addition per unit weight of electrode. Previously, a larger titanium addition to a tungsten-base electrode prevented melting entirely⁽¹⁾. The

consumption rate for VA-82 was quite slow (see Table 5 and Figure 10), even with a 6000 ampere melting current. The average furnace pressure was 0.015 microns, the lowest ever recorded while melting, which indicated that possibly the small amount of titanium present was having a desirable effect. The as-cast grain structure shown in Figure 11 was quite coarse, reflecting both the purification obtained by the titanium and the retarded melting rate.

It appeared that additional titanium in the electrode could not be transferred to the ingot, and any attempts to do so would result in a slower melt rate and a coarser as-cast structure. Therefore, ingot VA-89 was melted from an electrode containing both 0.04 percent titanium and 0.12 percent zirconium. The macrostructure of this ingot is shown in Figure 11. The grain size is smaller than that found in VA-82 and coarser than that found in VA-85. The presence of zirconium has offset the grain coarsening effect resulting from the titanium addition so that the as-cast structure resembles the "standard" W+0.6Cb sections shown in Figure 9. Processing and tensile data are discussed later.

Rockwell A hardness data for ingots produced in Phase I through III are shown in Table 9. The R_a hardness averaged 68.8, 68.3 and 65.5 for center, mid radius, and edge, respectively. The alloying additions have had little if any effect on the room temperature hardness, and average hardness appears to be a poor indicator of the purity, grain size, alloy content, extrudability, or any other properties of the W+0.6Cb alloy. The decrease of ingot hardness from the center to the edge of the ingot is contrary to observations of hardness variation described in other investigations (1,4) although the range of hardness values is about the same.

VI. MICROSTRUCTURES AND INGOT CHEMISTRY

Photomicrographs of the as-cast structure are shown in Figures 12 to 18. It is apparent in some cases that minor alloying elements, different powder lots, and differences in electrode consumption rates have an effect on microstructure, but it should be pointed out that differences in structure are sometimes the result of variances in electropolishing and etching technique. Specimens were often difficult to prepare so that significant differences between samples could be demonstrated. For instance, the electropolishing and etching procedure used on samples from ingot VA-82 was unsatisfactory for preparing samples from VA-81, probably because of the small amount of zirconium present, and VA-81 samples showed high relief and heavy pitting.

Some of the structures shown in Figures 12 through 18 closely resemble those published by other investigators (4,6). Many samples contained grains which exhibited a fine network of subgrain boundaries at 100 to 250X. This is shown clearly in Figure 12, and to a lesser extent in Figures 13, 14 and 16. Similar structures were not sought and photographed in other samples to avoid needless duplication. The subgrain boundaries, when magnified, appeared as rows of closely-spaced dislocation pits, which delineate the low angle intersection of lattice planes. Such an occurrence is attributed to a force sufficient to cause some deformation of the grain, and cooling stresses apparently produce forces sufficient to achieve this. Perhaps all grains exhibit this condition to some degree, but it is not evident because they are not favorably oriented with the polishing plane.

All samples contained randomly distributed prismatic "etch pits". The writer hesitates to ascribe these pits to a specific alloying addition or to general impurity content, as the "pit density" or pits per unit of area seems related to the amount of etching given a particular sample. It was noted that lightly etched samples showed relatively few pits, and the amount of pits increased after additional exposure to etchant. One may observe that samples containing fairly large amounts of carbon were less inclined to show pits than other specimens.

The "cleanest" structure was exhibited by the sample from VA-82, which contained a small amount of titanium (Figure 18), although the structure of VA-81 and VA-85 containing small amounts of zirconium (Figure 17), and VA-86, VA-90, and VA-92 (Figure 15) which were melted from electrodes containing excesses of oxygen, may be rated as "close seconds". VA-90 is not shown because the structures closely resembled those shown for VA-86 and VA-92.

Photomicrographs in Figure 16 of the material produced during the melting rate study disclosed a difference in structure at 250X, where it may be observed that ingot VA-80 contains more inclusions. The spots in the grains indicate the location of a foreign substance that was present prior to electropolishing. A minute quantity of unidentified grain boundary deposit is evident in the 2000X photos of VA-80 which is not noticeable in the structures of VA-78 and VA-79. What appears to be wide grain boundaries in the other photos is actually shadow resulting from preferential grain etching and oblique lighting.

Grain boundary deposits are very much in evidence in Figures 12, 13, and 14. Although the electrode material for

ingots VA-67 and VA-68 was purchased as low carbon material, it was soon apparent that the carbon content was in excess of the maximum capable of being retained in solid solution. None of the ingots that exhibited a grain boundary precipitate could be extruded. Ingots produced from electrodes of higher carbon content showed greater amounts of precipitate, as expected. The addition of titanium to the high carbon material produced not only an additional volume of deposit, but some precipitated material within the matrix. This is shown in the lower right hand photo in Figure 14. The dark area surrounding each particle indicates where material was removed during polishing and/or etching. Additional polishing or etching would have removed the material holding the particles in place and only voids would have remained.

If 15 percent molybdenum were the major alloying constituent, instead of 0.6 percent columbium, the general appearance of the microstructures in Figures 12 through 18 would have been essentially the same (6), except perhaps where excesses of oxygen existed in the electrodes.

Chemistry data on electrodes and ingots are shown in Tables 2, 3, 6, 7, and 8. Many of the observations, theories, and conclusions of this investigation hinged upon the sophistication of certain analytical techniques to show compositional variations resulting from exposing reactable elements to the environment created by melting tungsten in a vacuum furnace. Reliable thermodynamic data are available to indicate the reaction direction, even though certain assumed conditions of equilibrium are not even closely approached under actual conditions of melting. Other investigations (1,3) have confirmed some of this information.

A survey of analytical techniques and results (5,6,8) presented a fair indication of the results that may be expected when portions of a sample are analysed in several independent laboratories. The data in Tables 7 and 8 show considerable variation, particularly in the carbon analyses, and any indications pointing to loss or gain of interstitial elements resulting from the arc melting step were masked by the inability to obtain satisfactory analytical results. While some variation may be attributed to analytical error, most of the discrepancy can be traced to the method of obtaining samples from the electrodes.

Electrode samples were obtained by tapping the bar lightly with a small ball peen hammer so as to produce a row of small dents around the circumference of the bar, approximately $\frac{1}{8}$ inch from the end. The process was continued until a $\frac{1}{8}$ inch slice broke neatly from the electrode. About

a quarter of the slice was submitted as a single fragment for analysis and the balance was retained in case additional analysis became necessary.

Samples from electrode stubs, shown in Figure 19 were obtained in a similar manner, but care was taken not to include material which had obviously liquified, as solid state reactions were of particular interest. Inasmuch as the surfaces surrounding the stub samples had been wet by columbium, it was safe to assume that the samples submitted had been heated to at least 2450°C (4400°F).

Ingot samples were obtained according to the diagram on Figure 5. They were cut from the mid radius location with a silicon carbide wheel using a large stream of water as a coolant. It is not likely that sample contamination occurred during the cutting operation.

Although oxygen analyses were not always in reasonable agreement, residual quantities of this element in the ingot did not appear to adversely affect the workability of the arc cast material, so some effort was directed toward resolving the question of reproducibility of carbon results. It was found that, except for the extreme ends of the electrodes, carbon contents were fairly uniform along the length of the bars. The greatest difference in carbon content existed through the cross-section, and this condition was believed to have been caused by the hydrogen sintering operation. Exterior surfaces of high carbon electrodes contained a relatively small amount of carbon, and carbon content increased as samples were obtained closer to the center of the bar. More meaningful results could have been obtained if samples of uniform thickness were cut at least 1 inch from the end of each bar, and if it were specified that the entire slice should be granulated and blended before removing a sample for analysis. This procedure may have made oxygen analysis difficult because the chemist prefers a solid sample to minimize contamination.

Notice in Table 7 that nitrogen and hydrogen levels show a general tendency to be higher in the as-cast material than in the electrode material. This trend has been noted in another study (4). Perhaps essential differences in physical characteristics of sintered material as compared to arc melted material should be considered when applying certain analytical techniques.

The data in Table 6 show that columbium was generally well within specified limits, and also that predictable amounts of zirconium could be found in the ingots. It was

surprising to discover that fairly large amounts of titanium in the electrodes were almost completely eliminated by the arc melting step. Spectrographic analysis showed that most of the trace impurities were close to or below the minimum detectable limit and the efficiency of the arc melting process in removing these elements could not be determined.

VII. PRIMARY BREAKDOWN AND SUBSEQUENT EVALUATION

A. Extrusion

Extrusion is the only conversion process that can be relied upon to convert arc cast tungsten base billets into wrought form with reasonable success. All extrusions for this program were produced in the 600 ton high-speed Lombard horizontal press which is located at ASD,

Fourteen of the seventeen ingots produced during the course of the program were machined into extrusion billets and nine of these were extruded successfully. All of the ingots that failed to extrude contained more carbon than those that extruded and all exhibited a grain boundary precipitate under high magnification.

Ingots produced in the 3½-inch mold under the various conditions of melting were free of surface defects to the extent that satisfactory extrusion billets 2.945 ± .005 inches in diameter could be machined. The presence or absence of defects in ingots and billets was determined visually.

Ingots containing excess carbon were no more difficult to machine than any of the others, and generally exhibited better as-machined surfaces. Ingots that were made from high-oxygen electrodes generally exhibited the worst as-machined surfaces. These surfaces are compared in Figure 20. Ingots made from high oxygen electrodes showed a tendency to chip easily and the pressure of machining would always cause the condition shown in Figure 20. The microstructures show no concentration of a second phase at the boundary, nor do analytical results indicate that oxide levels differ from the average, yet a difference in properties is noted as early as the billet machining stage.

Extrusion data are summarized in Table 10 and all successful extrusions are shown in Figure 21. The "K" factor values listed in Table 10 show the "extrudability index" for the W+0.6Cb alloy by establishing a relationship between billet temperature, lubrication, extrusion pressure, and extrusion ratio. "K" factor values were obtained from the following equation:

$$K = \frac{P}{A_c \ln \frac{A_c}{A_x}}, \text{ where}$$

- K = extrusion constant, in psi
- P = total force on press ram, in pounds, required to initiate extrusion
- A_c = cross-sectional area of container, in square inches
- A_x = cross-sectional area of extrusion, in square inches

Since a 3.062 inch container was employed for all extrusions, the above equation may be simplified by combining constants to:

$$K = 118 \frac{\text{tons}}{\log \text{ extrusion ratio}}$$

In order to reduce the number of extrusion variables and thereby provide for better evaluation of arc melting variables, the billet length, extrusion temperature and extrusion ratio were held constant within practical limits. A nominal billet length of 5 inches, an extrusion temperature of 3800°F, and a reduction ratio of about 6.5:1 were found to be workable parameters for the W+0.6Cb alloy. Round orifice dies were employed to insure more uniform deformation of material.

The billet from ingot VA-68 would not extrude under the above conditions, and upon examination of the microstructure of the partially deformed billet, it appears that the material could not have been coaxed through the die under any conditions. Grain boundary separation was so severe that the billet crumbled when clamped for sectioning. The material surrounding the grains is evident even at low magnification, as can be seen in Figure 22. Notice that this deposit is apparently not present in structures from ingot VA-67, shown in Figure 12. The material does not uniformly envelop each grain in Figure 22. It was liquid at extrusion temperature and forced into available openings when the grains separated under the pressure applied by the extrusion press. All ingots made from high carbon electrodes in Phase II reacted similarly, although billet disintegration was never as

severe as it was with ingot VA-68. A typical unextruded billet is shown in Figure 20, and all other billets which failed to extrude resemble this billet very closely. Heating to 4200°F and reducing the extrusion ratio to 3.0:1 did not produce the slightest improvement.

The grain boundary deposit shown in Figure 22 was present in all unextruded ingots, although structures from ingot VA-87 required 2000X magnification for positive identification of the deposit.

The specific composition of this material is not known. It is translucent and appears reddish brown and amber under carbon arc illumination. "Miniature probe" analysis detected iron, and samples which were cut with an abrasive wheel, using water as a coolant, were observed to develop a rust-colored stain around exposed crack surfaces. Also, a stylus was used to break off some of the deposit which was exposed by drastically over etching the sample, and these particles were attracted to a magnet. However, the spectrographic analysis (Table 6) does not indicate a high concentration of iron in any of the ingots that failed to extrude, and the single conspicuous element is carbon. While it is not evident from the photomicrographs, the grain boundary deposit does not appear to consist of tungsten carbide alone, but rather a solution of carbides, including iron and possibly columbium.

Liquid at the grain boundaries should not prevent the material from passing through the die, and it should emerge as a quantity of individual grains if liquation were the only factor preventing generation of high-integrity extrusions. High carbon levels apparently contribute greatly to the ability of individual grains to resist deformation at elevated temperature.

A certain amount of carbon in the W+0.6Cb alloy is tolerable, and a carbon level, higher than that found in the easily extrudable billets but lower than that in the unextrudable billets, must exist which would produce better high temperature properties. This level was not determined. The presence of molybdenum in tungsten apparently allows carbon to be present in larger quantities while still permitting satisfactory deformation by extrusion and other methods^(7,9), and carbon levels used for property improvement in W-Mo alloys are in a range suitable for analytical control⁽⁸⁾. Data from this investigation indicate that carbon additions to W+0.6Cb must be limited to small concentrations where techniques for analytical control may not be satisfactory.

Heat treatment of the as-cast material was suggested early in the program as a means to promote some diffusion of troublesome constituents, so the billet blanks were preheated slowly to 1000°F

in air in an electric furnace to prevent cracking resulting from thermal gradients below the transition temperature. The billets were transferred to another furnace and allowed to remain at 2200°F for 1 hour in an argon atmosphere. The blanks were then returned to the 1000°F furnace and slowly returned to room temperature. Oxidation was of no concern because of the amount of material removed when the blank was machined into a billet. The effect of heat treatment on hardness is shown in Table 9.

Billet blanks from ingots VA-78, VA-79, VA-81 and VA-82 were subjected to the treatment just described, and all were extruded without difficulty, as can be seen in Table 10. Ingot VA-83 was long enough to produce two five-inch billets, as mentioned previously, and this offered an opportunity for experimentation. The upper section of this ingot was heat-treated, the lower section was not. If the billet heat treatment step was the factor enabling successful extrusion of the W+0.6Cb alloy, then billet VA-83U had the best chance to produce an extrusion, so it was scheduled before billet VA-83L. VA-83U did not extrude, however, and the unextruded billet is shown in Figure 20. The likelihood of extruding VA-83L under the same conditions was small, and, as mentioned earlier, heating to 4200°F and using a 3:1 die did not produce results.

Heat treatment is apparently ineffective in rendering an otherwise unextrudable billet of W+0.6Cb alloy capable of being extruded, and this practice was discontinued. Universal Cyclops (4) heat treated billets of unalloyed tungsten to 3100°F for two hours without obtaining any significant effects.

The as-extruded surfaces of the material exhibited in Figure 21 ranged from excellent to poor. The best and worst surfaces are shown in Figures 23 and 24. The condition shown in Figure 24 was observed only when extruding material originating from electrodes with a high oxygen content. Extrusion surfaces could have been improved by manipulation of arc melting and extrusion variables, however extrusion surface quality was secondary to the workability determination, and parameters were maintained as previously established in order not to invalidate comparisons essential to the program.

Some extrusion data are listed on the following page for W+0.6Cb billets produced by outside suppliers and extruded at 3800°F by the ASD facility for another program(10). Data are shown to compare material extrudability ("K" factor) as it might be influenced by melting with different parameters in different furnaces, however the values listed are reasonably uniform.

<u>Ingot Number</u>	<u>Extr. No.</u>	<u>Billet Weight (Pounds)</u>	<u>Billet Length (Inches)</u>	<u>Ratio</u>	<u>Breakthrough Pressure (Tons)</u>	<u>"K" Factor (psi)</u>
<u>ASD</u>						
VA-78	935	22.8	4.81	6.4:1	515	75,600
VA-79	936	22.1	4.94	8.3:1	590	76,000
VA-81	946	23.2	5.13	6.4:1	530	77,700
VA-82	947	23.3	5.06	6.4:1	495	72,600
VA-86	956	23.0	5.00	6.4:1	500	73,200
<u>UNIVERSAL CYCLOPS</u>						
KC1138A	752	21.8	4.75	4.3:1	420	79,000
KC1138B	753	21.8	4.69	8.0:1	520	80,500
KC1146A	755	22.0	4.75	4.4:1	480	90,500
KC1146B	756	20.7	4.25	5.7:1	530	82,000
KC1145B	762	21.8	4.75	4.4:1	480	91,000
<u>WAH CHANG</u>						
31015T	992	20.3	4.31	4.3:1	410	76,000
31192B	995	22.3	4.75	6.8:1	450	64,000
<u>OREMET</u>						
OM1523-3	997	21.6	4.63	6.7:1	560	82,000

Extrusions were sandblasted to remove adhering lubricant and Sil-O-Cel, and marked off for evaluation sectioning according to the diagram in Figure 25. The nose, center, and tail discs were used for hardness determination and microexamination, and the material between these discs was used for swaging and forging stock, with the material having the best surface chosen for swaging.

Samples of extrusions 956 and 974 were cut longitudinally for macroexamination to determine the effect of the original ingot grain size on the wrought structure. Both transverse and longitudinal sections are compared in Figure 26 and the differences are obvious. To compare the transverse and longitudinal sections of ingots from which these extrusions originated, turn to Figure 8 and examine VA-86 and VA-92.

Extrusion hardness data are listed in Table 11. As was the case with ingot hardness, there was little variation, although trends are discernible. The center sections average softer than the nose and tail samples. Tail samples, particularly near the

edge, contain the hardest portion of the extrusions. This region was subjected to contact with the relatively cold container and cold follower block longer than any other portion of the bar.

Microstructures of all extrusions are shown in Figures 27 through 31. Recrystallization is evident in varying degrees in all center slices. The tendency of the W+0.6Cb alloy variations to recrystallize may be estimated roughly from a comparison of the microstructures. The center samples show structure representative of most of the bar. The nose samples suffered some heat loss, and were subjected to less deformation, while the tail samples were considerably cooler than the material preceding them through the die for the reasons given in the previous paragraph. Compare Figures 27 and 28. Figure 27 shows samples of "standard" W+0.6Cb alloy extruded at 6.4:1 and 8.3:1. Most of the recrystallization occurred in the center sample, while significantly less was present in the nose sample and none occurred in the tail sample. In Figure 28, extrusion 946 originated from ingot VA-81 which contained 0.06 percent zirconium, and the center sample is only slightly recrystallized, while no recrystallization has occurred in either nose or tail sample. Extrusions 955 and 964 in Figures 29 and 30 were similar in composition and showed similar recrystallization tendencies. Extrusion 947 (Figure 28) originated from ingot VA-82 which contained a small amount of titanium in the electrode. It shows a strong tendency to recrystallize, as even the nose and tail sections show considerable quantities of new grains. Some original as-cast structure is present in the nose sample, attesting to the small amount of deformation in the center of the nose of this extrusion. Since only a small fraction of the titanium added to the electrode could be detected in the ingot, it is apparent that an increase in ingot purity occurred as titanium was removed along with those residual impurity elements that retard recrystallization.

Extrusions 956, 965 and 974 are shown in Figures 29, 30, and 31. This material was produced from ingots VA-86, 90 and 92 which were made from high oxygen electrodes. The structures resemble those from extrusions 935 and 936, except for a greater tendency to recrystallize. The similarity of structure between extrusions 947 and 956, and the low "K" factor values (see Table 10) suggest that both of these extrusions were made from ingots of higher than average purity. Samples of extrusion 965 (Figure 30) show no recrystallization. An excessively long billet transfer time caused by difficulty in inserting the billet into the container allowed the billet to lose considerable heat, and the temperature of the extrusion was below that required for recrystallization to begin. Although the tail sample of this extrusion showed a crack, the balance of the bar was sound. Subsequent evaluation indicated that the recrystallization behavior of extrusion 965 was similar to extrusions 935, 947, and 956.

B. Forging

Samples for forging were cut from the extrusions according to the diagram on Figure 25, using a silicon carbide cut-off wheel (Allison C120JRA). Some of these samples are shown in Figure 32. Inasmuch as this material was known to be partially recrystallized, all specimens were heated for 1 hour at 3200°F (1760°C) in argon to insure that recrystallization was complete. Metallographic examination of the specimens after forging showed that the annealing procedure produced the desired structure in samples containing zirconium, but the recrystallized grain size was somewhat large in other specimens.

Some defects evident in the as-extruded surface still remained after machining away a .060-inch layer of material to obtain the 1.125-inch diameter forging sample. Other machined samples seemed defect free, as determined visually, however nearly all forgings showed ruptures of the type displayed in Figure 32. These samples were oriented specifically to show defects and were stacked in the order of removal from the extrusion. It is uncertain as to whether the defects were present in the ingot, were caused by billet machining practice, or were a result of extrusion practice. Data obtained from forging studies are listed below.

<u>Samples</u>	<u>Height (in.)</u>		<u>%</u>	<u>R_a Hardness</u>		
	<u>Mach'd</u>	<u>Forged</u>		<u>Red.</u>	<u>Extr'd</u>	<u>Annl'd</u>
935	2.251	1.050	53	70.0	68.6	72.6
946	2.256	0.995	56	70.7	69.6	72.6
947	2.250	0.975	57	68.7	69.0	73.4
955	2.253	1.047	54	69.3	70.1	71.5
956	2.260	1.021	55	69.7	69.4	72.3
964	2.262	1.020	55	72.0	69.9	71.7
965	2.252	1.000	55	72.6	72.9	72.1

C. Recrystallization

The forged samples discussed in the previous section were cut into coupons measuring approximately 0.50 x 0.40 x 0.25 inches and subjected to various annealing temperatures for various times to establish a time-temperature relationship for the beginning and ending of recrystallization for wrought samples of W+0.6Cb (extrusion 935). Samples were heated in a carbon tube furnace in argon, and were placed on a molybdenum

sheet to prevent contamination from the carbon "boat". The effect of heat-treatment on structure was determined metallographically.

The time-temperature plot shown in Figure 33 was obtained as a result of this study. It was patterned after similar work by Bechtold⁽¹⁾ on molybdenum, and may be compared to data obtained in the previous program on the 92W-6Mo-2Cb alloy⁽¹⁾. Figure 33 tentatively establishes hot and cold working temperatures and approximates the permissible time at temperature for stress relief anneal without recrystallization.

Forged samples of extrusions 946 and 947 were annealed and the results compared to the "standard" W+0.6Cb extrusion (935) to demonstrate the effects of zirconium and titanium on recrystallization behavior of forged samples. It was expected that the slope of the lines indicating the beginning and end of recrystallization would be about the same for each alloy, however, it will be noted in Figure 33 that such was not the case. Figure 34 shows samples of each extrusion that were heated for 150 minutes at 2800°F (1550°C) and 20 minutes at 3200°F (1760°C). Recrystallization had just begun in samples 935 and 947 at the lower temperature, and had not begun in sample 946, containing 0.06% zirconium. At the higher temperature, recrystallization is complete and grain growth had occurred in samples 935 and 947, while sample 946 is only partially recrystallized. It is felt that a more uniform as-forged grain size can be obtained by varying annealing conditions to suit the characteristics of each alloy. Work is still in progress, and additional results from this study will be contained in a report to be published by ASD.

D. Swaging

A portion of each extrusion (except 974) was submitted to the Westinghouse Materials Manufacturing Division, Blairsville, Pennsylvania, for swaging in the Torrington 1406 machine. The section of extrusion between the nose and center samples (Figure 25), measuring about 10 inches long and 1.22 inches in diameter, generally exhibited the best surface and was used for the swaging study. Five die sizes were employed to swage the bars to .625-inch stock which was considered suitable for machining into tensile specimens.

Five of the extrusions had to be heated to at least 2800°F (1550°C) before swaging could be accomplished, but the three bars containing zirconium could not be swaged at

this temperature and were heated to 2900°F (1600°C) so that they could be worked satisfactorily. The extrusion sections were first swaged with a 1.125-inch die (15% reduction) and then with a .947-inch die (30% reduction). Samples were removed from each bar and the transverse microstructure of these samples is shown in Figure 35. Up to this point the material had been subjected to a 40% reduction in area from the extruded cross-section, and comparing these microstructures with those of the as-extruded bar (Figures 27 to 30), it may be observed that some additional recrystallization had occurred in each specimen. The relative tendency for each material to recrystallize during swaging follows the trends indicated by the center samples of the extrusions.

All samples (except 936) were annealed at 3100°F (1700°C) in a hydrogen atmosphere. The bars from extrusions 946, 955, and 964 were held at temperature for 90 minutes and the balance of the material was annealed for 75 minutes. The bars were then swaged using .850, .750, and .627 inch dies, giving a total reduction in area of 56 percent from the annealed .947-inch bars. The transverse microstructures of the samples removed from the bars after the final swaging pass are shown in Figure 36. Sample 936, which was not subjected to the annealing cycle, had completely recrystallized during heating to the swaging temperature. Samples from bars 946, 955, and 964 that contained minor amounts of zirconium exhibit a fine grain size, even though they were held at annealing temperature somewhat longer than the other bars. Compare the wrought microstructures in Figure 36 with the ingot macrostructures in Figures 8, 9, and 11.

E. Tensile Testing

Seven of the eight samples of swaged bar were machined into standard vacuum creep-rupture specimens (Figure 37). The microstructures in Figure 36 are considered representative of the structures in the tensile specimens. The specimen from bar 956 broke during the finish-machining step, and it was noted later, during removal of samples for microexamination, that the rest of the bar contained a number of longitudinal cracks. The cause of these internal fractures was not determined.

The data from the remaining samples are shown in Table 12. The values obtained from samples 935, 936, 947, and 965 are considered typical for the W+0.6Cb alloy under the conditions of testing, however the properties exhibited by samples 946, 955, and 964 have been improved by the presence of zirconium and titanium. Compare the relative

stress values in Table 12 with the relative "maximum force" and "K factor" values in Table 10.

Considering the property improvement obtained by adding zirconium and zirconium plus titanium to W+0.6Cb, it appears that this material warrants further investigation. More zirconium could have been added before extrusion pressures become high enough (about 600 to 620 tons) to stall the ASD press, and if this had occurred, billets could have been heated to a higher temperature and/or the extrusion ratio could have been reduced.

VIII. INTERNAL SUPPORT

Nine heats of the 92W-6Mo-2Cb alloy have been prepared under the "Internal Support" program of this contract. Figure 38 shows threaded electrode sections of 94 tungsten - 6 molybdenum to which 2 percent columbium will be added in the form of wire. The 94W-6Mo material has a better green strength than pure tungsten and electrodes may be obtained in consistently long lengths. Pure tungsten electrode sections are shown in Figure 3. The glossy finish simplifies the task of keeping the exterior free of greasy fingerprints and other matter. The melting characteristics of the most recent lot of electrodes are about the same as obtained from the previous lot, although 5800 amperes are now used for melting instead of 5500, in an attempt to obtain better ingot surfaces.

Poor extrusion surfaces have become a serious problem with the 92-6-2 alloy in the present material evaluation program. The defects are believed to be a function of ingot surface and/or arc melting practice. Extrusions produced from ingots melted during the previous program⁽¹⁾ exhibited better surfaces and the only extrusion defect of similar magnitude to the ones that are currently the center of attention was found in an extrusion from an ingot melted with only 4500 amperes.

An example of an unsatisfactory ingot surface is shown in the right hand photo of Figure 39 and is the result of both insufficient stirring and electrode camber. The opposite side of this ingot resembles the photo on the left, the surface of which is considered satisfactory, but not good. Ingot defects which extend deep enough to preclude their removal by machining to billet diameter produce the surface effect shown in the bottom photo of Figure 39. Improved ingot and billet surfaces can be obtained by increasing the stirring current, increasing the melting current, and by increasing the mold diameter. The latter alternative will result in greater material loss because of additional machining required to achieve the same billet

diameter, but may produce superior extrusions and ultimately larger useable yields.

Melting data for internal work are summarized in Table 13 and electrode melting rate vs. input is plotted in Figure 40 as an extension of data obtained on this alloy during the previous arc melting program.

Melting of columbium base alloys containing up to 5 percent molybdenum and tungsten is also part of the internal support program. Two-inch diameter molds were designed to produce small ingots because of the expense of columbium base alloys. One ingot of pure columbium was produced with this equipment and is shown in Figure 41. Examination of sections of this ingot showed that it was excellent, but the melting parameters leave much to be desired. The minimum current required to maintain a stable arc was 1600 amperes and the electrode was consumed very quickly at this power level. When 1500 amperes or less was used, the arc would climb the electrode and stabilize between the electrode adapter and stinger rod seal extension, a condition that would soon cause penetration of the furnace shell.

Two ingots of pure tungsten have been made in the 2-inch molds from electrodes measuring about 1 inch in diameter. Satisfactory electrode consumption was achieved at 3200 to 3400 amperes and no mold damage occurred. No references could be located describing successful production of similar size ingots using DC straight polarity as a power source.

The internal support program calls for columbium-base alloys containing various amounts of molybdenum and tungsten. The original intent was to add molybdenum and tungsten wire to a central electrode of pure columbium, however the minimum electrode melting rate is so rapid that insufficient time is available for the melting and solution of tungsten. The melting points of columbium and molybdenum are close enough that no such problems are anticipated.

Columbium alloys of the desired composition were obtained in billet form for extrusion into 1-inch and 3/4-inch bars. Some of these pre-alloyed bars will ultimately be used as electrodes to produce 2-inch ingots of columbium base alloy.

IX. EQUIPMENT MODIFICATIONS

The molds designed to produce 2-inch ingots of columbium base alloy are shown in Figure 42 along with other items necessary to adapt the smaller mold to existing equipment. The

molds are machined from 3-inch O.D. x 2-inch I.D. OFHC copper tubing and a 6-inch flange is silver soldered to the top. The molds were made as short as possible (9½ inches) to minimize the effect of the small cross-sectional area through which any evolved gases must pass as they are removed from the region of melting. The adapter plate covers the 8-inch opening in the furnace and permits use of the 6-inch mold flange. The liner fits into the water jacket (Figure 2) and reduces the annular space of the jacket to a .125 inch clearance around the smaller mold. The mold bottom was made longer than necessary so that the existing conductor tube can be used with both mold sizes.

Four inch diameter molds have been modified and a new water jacket was machined to produce 4-inch ingots of 92-6-2 alloy for the extrusion contract. Design features are identical to those employed for the 3½-inch molds used previously, and ten 4-inch ingots of 92-6-2 alloy have been melted successfully.

X. CONCLUSIONS

1. Sound 3½ and 4-inch diameter tungsten base (W+0.6Cb and 92W-6Mo-2Cb) ingots can be produced consistently, with no difficulty from mold burn-through, by the melting techniques developed in this investigation.

2. The size of columnar grains in arc cast W+0.6Cb ingots is decreased by rapid melting rates and by minor additions of zirconium (0.06 to 0.12%) and carbon (50 to 250 ppm). The ingot grain size is increased by slow melting rates and by minor additions of titanium (0.04%) and oxygen (500 to 1000 ppm).

3. Carbon content significantly affects the extrudability of the W+0.6Cb alloy, and ingots containing more than 50 ppm of carbon could not be extruded. Oxygen (500 to 1000 ppm) is tolerable in sintered tungsten electrodes as nearly all of it is eliminated during arc melting.

4. Minor additions of zirconium (0.06 to 0.12%) improved the elevated temperature tensile properties of the W+0.6Cb alloy.

XI. REFERENCES

1. Reimann, G. A., Vacuum Arc Melting of a Tungsten Alloy (Tungsten - Molybdenum - Columbium); Westinghouse Electric Corporation, ASD-TDR-62-781, August, 1962.
2. Smithells, Colin J., Metals Reference Book, Vol. II, Butterworths Scientific Publications, London, 1957, p. 587.
3. Investigation of the Properties of Tungsten and Its Alloys; Union Carbide Metals Company, Division of Union Carbide Corporation, Niagara Falls, N.Y. WADD-TR-60-144, May, 1960.
4. Schoenfeld, W. J., Tungsten Sheet Rolling Program; Universal-Cyclops Steel Corporation, AMC Interim Report 7-827 (II), April - August, 1961.
5. Lake, F. N. and Breznyak, E. J., Tungsten Forging Development Program; Materials Department, Tapco Group, Thompson Ramo Wooldridge Inc., Cleveland, Ohio. AMC-TR-7-797 (I), September, 1960.
6. Ibid., AMC-TR-7-797 (II), December, 1960.
7. Ibid., AMC-TR-7-797 (III), March, 1961.
8. Report of the Subpanel on Analytical Techniques, Refractory Metals Sheet Rolling Panel; Materials Advisory Board of the Division of Engineering and Industrial Research, Washington, D.C., November, 1961.
9. Semchyshen, M., Barr, R. Q., and Chesmar, G. G., Development of Workable Molybdenum and Tungsten Base Alloys; Climax Molybdenum Company of Michigan, ASD-TDR-62-508, June, 1962.
10. Carnahan, D. R. and Visconti, J. A., The Extrusion, Forging, Rolling, and Evaluation of Refractory Alloys; Westinghouse Electric Corporation, ASD-TDR-62-670, October, 1962.
11. Bechtold, J. H., Recrystallization Applied to Control of the Mechanical Properties of Molybdenum; Transactions, American Society for Metals, Vol. 46, 1954.

TABLE 1
ELECTRODE CHARACTERISTICS

Electrode Number	Powder Lot	Density (%)	As Rec'd		Camber (in.)	Machined		Diameter		Lb./In.	Ingot
			Wt. (lb.)	L (in.)		Wt. (lb.)	L (in.)	Max. (in.)	Min. (in.)		
06208-2	3388	92.6	30.6	26.88	1/16	29.9	26.63	1.505	1.492	1.12	VA-68
06208-6	3388	92.7	32.6	27.75	1/16	31.9	27.38	1.520	1.497	1.16	VA-67
09115-1(a)	3388	92.9	41.0	28.00	0	34.4	27.63	1.632	1.620	1.25	VA-83
09115-2(b)	3388	93.1	39.1	27.38	----	22.2	20.63	1.703	1.247	----	VA-66
09115-4(a)	3388	93.6	43.0	27.88	0	34.6	27.63	1.625	1.615	1.25	VA-83
09297-4	3782	92.6	29.8	22.75	1/16	27.4	21.75	1.640	1.610	1.31	VA-81
09297-5	3782	92.4	25.7	19.50	3/32	22.3	17.63	1.655	1.625	1.32	VA-80
09297-6	3782	92.0	18.6	14.63	3/32	17.7	13.63	1.646	1.605	1.27	VA-81
09297-7	3782	92.4	17.6	13.25	1/16	16.6	12.50	1.637	1.617	1.33	VA-82
09297-8	3782	92.2	31.5	23.38	1/16	28.9	22.25	1.685	1.648	1.34	VA-78
09297-9	3782	92.4	26.0	19.50	1/16	23.6	18.38	1.660	1.616	1.33	VA-80
09297-10	3782	92.2	32.3	24.00	1/16	30.9	22.75	1.708	1.640	1.34	VA-78
09297-11	3782	92.5	28.7	22.50	1/8	26.4	21.13	1.645	1.594	1.27	VA-82
09297-12(c)	3782	92.6	30.0	23.00	----	25.4	19.50	1.632	1.622	1.30	VA-85
09297-13(c)	3782	92.6	30.0	23.00	----	24.6	19.25	1.638	1.613	1.30	VA-85
09297-14	3782	92.0	29.4	23.00	1/16	27.0	21.75	1.640	1.610	1.28	VA-79
09297-16	3782	92.5	28.9	22.88	3/32	27.3	22.00	1.630	1.585	1.26	VA-89
11234-1	M621137	92.6	30.8	21.88	1/8	29.0	21.00	1.705	1.665	1.41	VA-88
11234-2	M621137	92.6	31.7	22.63	1/16	29.6	21.38	1.715	1.655	1.40	VA-88
11234-3	M621137	92.6	32.3	23.50	1/32	30.0	22.13	1.678	1.647	1.37	VA-91
11234-4	M621137	92.6	32.2	23.50	3/32	30.6	22.63	1.705	1.650	1.37	-----
WC-1	WC8-111	89.7	33.1	25.38	3/16	30.6	23.88	1.670	1.622	1.30	VA-86
WC-2	WC8-111	89.7	35.5	26.00	1/4	33.7	25.13	1.750	1.660	1.36	-----
WC-3	WC8-111	89.5	33.1	24.25	5/16	30.8	22.94	1.758	1.670	1.36	-----
WC-4	WC8-111	89.8	33.2	23.63	7/32	30.2	21.80	1.787	1.709	1.40	-----
WC-5	WC8-111	89.7	35.6	26.13	5/32	33.1	24.75	1.711	1.637	1.37	VA-86
W3-1-C(c)	H1496	92.4	19.1	16.00	----	17.5	14.50	1.560	1.545	1.20	VA-87
W5-1-C	H1496	91.7	21.3	18.75	3/32	19.9	17.06	1.575	1.500	1.16	VA-87
W6-2-0	H2071	90.7	18.8	17.50	1/8	16.0	14.88	1.523	1.468	1.07	VA-90
W6-3-0	H2071	90.7	18.6	17.00	1/32	16.8	15.25	1.516	1.499	1.10	VA-90
W6-5-0	H2071	87.0	15.2	13.00	1/16	14.4	12.50	1.635	1.604	1.17	VA-92
W7-1-0(c)	H2151	92.4	21.6	19.25	----	19.7	17.88	1.496	1.460	1.12	VA-92
W7-2-0	H2151	93.2	14.3	13.50	1/16	12.4	12.00	1.450	1.400	1.06	VA-92

(a) Electrode machined to 1.625 for entire length.

(b) Electrode machined to 1.250 and 1.500.

(c) Electrode broken in shipment.

"W" electrodes supplied by Westinghouse Electric Corp., Blairsville, Pa.

"WC" electrodes supplied by Wah Chang Corp., Albany, Oregon.

All other electrodes supplied by General Electric Corp., Cleveland, Ohio.

TABLE 2

	SUPPLIERS' ANALYSES OF MELTING MATERIAL										R&D Metals (Columbium Wire)	
	General Electric		Wah Westinghouse (a)		Chang		W7		.063 & .125"			.091"
	06208	09115	09297	11234	WC	W3	W6	W7	.063 & .125"			
Carbon	50	135	*10	240	*30		23	18		*20	*30	
Oxygen	6*5	12*5	25*5	4*4	50	30	552	910		65	65	
Nitrogen	1*1	4*4	2*2	1*1	10	7	8	12		57	50	
Hydrogen	1*1	1*1	1*1	1*1	--	4	5.4	2.5		16	18	
Columbium	--	--	--	--	0.74%	.58%	.57%	.58%		--	--	
Aluminum	*10	*10	*10	*10	*10		10			*20	*20	
Boron	--	--	--	--	--	--	--	--		*0.5	*1	
Cadmium	--	--	--	--	--	--	--	--		*5	*5	
Calcium	*10	*10	*10	*10	*10		*10	15		--	--	
Chromium	*10	*10	*10	*10	*10		*10	10		*10	*20	
Copper	*10	*10	*10	*10	*10		*10	*10		--	--	
Iron	30	30	*10	10	25		20	20		*100	*100	
Hafnium	--	--	--	--	--		--	--		*75	*80	
Magnesium	*10	*10	*10	*10	*10		*10	*10		--	--	
Manganese	*10	*10	*10	*10	*10		*10	*10		*20	*20	
Molybdenum	60	60	40	70	25		25	20		*20	*20	
Nickel	*10	*10	*10	10	20		20	10		*20	*20	
Silicon	10	10	*10	*10	*10		*10	30		*75	*100	
Tantalum	--	--	--	--	--		--	--		560	560	
Tin	*10	*10	*10	*10	*10		--	--		--	--	
Titanium	--	--	--	--	--		--	--		*100	*150	
Vanadium	--	--	--	--	--		--	--		*200	*20	
Tungsten	--	--	--	--	--		--	--		*100	*200	
Zirconium	--	--	--	--	--		--	--		*500	*500	

General Electric analytical methods: carbon - conductometric; oxygen, nitrogen, hydrogen - vacuum extraction; metallics - spectrographic powder analysis. Wah Chang and R&D Metals analytical methods unavailable.

(a) Analysed by Le Doux Co., Inc. Analytical methods on Table 3.

All analyses reported in parts per million unless indicated otherwise.

*Indicates lower detection limit. Actual value lower than that shown.

TABLE 3
INDIVIDUAL ELECTRODE ANALYSES

	06208-8	09115-4	09297-4	09297-5	09297-8	09297-9	09297-10	09297-11	09297-14	WC-3	WC-4	11234-2	11234-3	W3-1C	W6-3-0	W7-1-0
C	93	47	21	17	22	27	29	27	38	36	67	49	125	50	23	18
O	18	5	9	13	5	2	13	10	6	8	9	25	20	30	552	910
N	4	7	10	10	9	4	9	8	15	7	4	13	8	7	8	12
H	3.3	2.9	1.1	1.7	1.2	1.2	1.3	0.9	1.4	6.6	4.5	4.3	5	4	5.4	2.5
Cb	--	--	--	--	--	--	--	--	--	.69%	.66%	--	--	.58%	.57%	.58%
Al	10	5	--	*5	--	--	--	*5	--	*10	*10	30	35	--	10	15
Ca	*10	*10	--	*10	--	--	--	*10	--	*10	*10	*10	30	--	*10	*10
Cr	10	*10	--	*10	--	--	--	*10	--	*10	*10	*10	*10	--	10	10
Cv	*10	*5	--	*5	--	--	--	*10	--	*10	*10	*10	*10	--	*10	*10
Fe	50	40	20	20	20	30	--	20	20	20	25	10	20	--	20	20
Mg	*10	*5	--	*5	--	--	--	*5	--	*10	*10	*10	*10	--	*10	*10
Mn	*10	*5	--	*5	--	--	--	*5	--	*10	*10	*10	*10	--	*10	*10
Mo	20	20	--	20	--	--	--	500	--	35	50	50	35	--	25	20
Ni	10	10	--	10	--	--	--	10	--	40	*10	*10	20	--	20	10
Si	20	20	15	15	15	15	--	20	15	*10	*10	*10	20	--	*10	30
Sn	--	*10	--	*10	--	--	--	*10	--	*10	--	*10	*10	--	--	--

302r

Analyses performed by Le Doux Co., Inc., Teaneck, N.J. Analytical methods: carbon - conductometric; oxygen - inert gas fusion; nitrogen - microkjeldahl; hydrogen - vacuum extraction; columbium - photo-colorimetric; others - spectrographic.

All analyses reported in parts per million unless indicated otherwise.

* Indicates that actual values are less than values shown, which are the lower limit of detection for the analytical method used.

TABLE 4

TYPICAL MELT RECORD OF W+0.6Cb

Ingot number VA-78
 Electrodes 09297-8(upper) 09297-10(lower)
 Electrode size 1.7 x 45"
 Mold size 3.5 x 18.5
 Starting pad weight 9.1 lb.
 Furnace starting pressure 0.006 microns

<u>Time</u>		<u>Amperes</u>	<u>Volts</u>	<u>Pressure (Microns)</u>	<u>Stirring (Amperes)</u>	<u>Electrode Travel (Inches)</u>	<u>Remarks</u>
<u>Min.</u>	<u>Sec.</u>						
0	10	3600	36	0.02	2	0	
1	10	4500	28	0.02	2	0	
2	30	5000	28	0.03	2	0	
3	15	5500	28	0.03	3	2	
6	00	5800	29	0.03	3	3	Stirring clockwise
8	50	5800	28	0.05	3	4½	
12	25	5800	28	0.04	3	6	
16	00	5800	27	0.03	3	8	
22	17	5800	28	0.03	3	12	
32	30	5800	28	0.02	3	21	
34	50	5800	28	0.03	3	23	
38	10	5800	28	0.02	1	26	
38	20	3400	26	0.02	1	--	Hot topping
39	10	2500	28	0.01	1	--	
39	50	-----	--	0.01	--	--	Power off

Ingot weight, 52.0 lb. (including pad)
 Electrode stub weight 17.2 lb.

TABLE 5
SUMMARY OF W+0.6Cb ARC MELTING DATA

Heat Number	Melting Current (amperes)		Average Arc Voltage	Kilo-watts	Average Stirring Current (amperes)	Pressure (microns)		Melting Rate (lb./min.)	Total Melt Time (min.)	Ingot Weight (lb.)				
	Start	Finish				Pre-melt	Max Avg			Gross Blank	Finished Billet			
VA-66	4000	4800	2500	28	134	3.0	.004	.05	.03	16.3	23.4	----	----	
VA-67	3800	5400	2500	28	151	3.0	.004	.10	.08	1.54	40.2	----	----	
VA-68	4000	5500	2500	26	145	0.5	.006	.09	.05	1.55	18.7	38.9	26.5	16.9
VA-78	3600	5800	2500	28	162	3.0	.006	.04	.03	1.21	39.8	52.0	30.0	22.8
VA-79	4000	6500	2500	28	182	2.5	.006	.06	.04	1.71	30.3	49.1	32.2	22.1
VA-80	4000	7200	7200	28	202	1.8	.005	.05	.08	2.57	15.0	45.0	----	----
VA-81	4000	6200	2500	28	174	2.8	.005	.06	.04	1.30	32.4	52.0	31.9	23.2
VA-82	4000	6000	2500	28	168	2.0	.004	.05	.015	0.75	53.8	49.2	31.5	23.3
VA-83	4800	6000	2500	28	168	2.0	.005	.10	.06	1.83	39.9	80.1	34.6U 31.5L	23.2 23.1
VA-85	4000	6000	2500	28	168	2.0	.004	.05	.04	1.35	38.5	55.9	33.7	23.2
VA-86	4000	5800	2500	28	162	2.0	.004	.04	.02	2.50	25.3	58.1	32.5	23.0
VA-87	4600	5800	2500	28	162	2.0	.005	.08	.06	1.93	26.0	48.0	32.3	23.1
VA-88	4500	5800	2500	28	162	2.0	.004	.05	.04	1.71	28.6	55.4	33.2	23.4
VA-89	4500	6000	2500	28	168	2.0	.004	.06	.03	0.74	56.1	50.5	32.5	23.1
VA-90	4000	5800	2500	28	162	2.0	.005	.10	.06	0.97	46.1	48.5	31.6	23.3
VA-91	4400	6000	2500	28	168	2.0	.005	.04	.03	0.63	74.0	57.3	32.2	23.0
VA-92	4000	5800	2500	28	162	2.0	.004	.20	.10	0.66	70.2	54.6	32.6	23.2

34

TABLE 6

W+0.6Cb INGOT ANALYSES

	<u>VA-67</u>	<u>VA-68</u>	<u>VA-76</u>	<u>VA-79</u>	<u>VA-80</u>	<u>VA-81</u>	<u>VA-82</u>	<u>VA-83</u>	<u>VA-85</u>	<u>VA-86</u>	<u>VA-87</u>	<u>VA-88</u>	<u>VA-89</u>	<u>VA-90</u>	<u>VA-91</u>	<u>VA-92</u>
Carbon	39	44	10	18	9	10	8	123	28	6	51	226	19	21	230	25
Oxygen	3	9	17	9	20	18	19	8	31	21	25	15	22	31	28	12
Nitrogen	6	8	22	14	10	26	28	13	9	6	12	20	5	18	19	12
Hydrogen	1.3	8.3	1.1	0.8	0.9	1.5	2.3	3.7	2.2	1.2	1.8	2.1	1.9	0.5	1.8	2.4
Columbium	0.55%	0.56%	0.68%	0.74%	0.69%	0.57%	0.48%	0.69%	0.59%	0.66%	0.57%	0.62%	0.57%	0.54%	0.56%	0.57%
Aluminum	--	--	--	10	10	35	15	*10	10	*10	*10	*10	*10	*10	*10	*10
Calcium	--	--	--	*10	*10	*10	*10	*10	*10	*10	*10	*10	*10	*10	*10	*10
Chromium	--	--	--	*10	*10	*10	*10	*10	*10	*10	*10	*10	*10	*10	*10	*10
Copper	--	--	--	*10	*10	*10	*10	*10	*10	*10	*10	*10	*10	*10	*10	*10
Iron	10	5	--	10	15	15	10	10	20	10	10	10	10	10	10	30
Magnesium	--	--	--	*10	*10	*10	*10	*10	*10	*10	*10	*10	*10	*10	*10	*10
Manganese	--	--	--	*10	*10	*10	*10	*10	*10	*10	*10	*10	*10	*10	*10	*10
Molybdenum	--	--	--	25	25	20	20	30	60	20	60	20	20	60	40	40
Nickel	--	--	--	--	*10	*10	*10	*10	*10	*10	*10	*10	*10	*10	*10	*10
Silicon	10	*5	--	10	15	15	10	*10	20	20	20	10	*10	20	10	30
Titanium	--	--	--	--	--	--	0.0015%	*10	*10	*10	*10	*10	0.0015%	*10	0.005%	*10
Zirconium	--	--	--	--	--	0.06%	--	*10	0.10%	*20	*20	*20	0.08%	*20	*20	*20

Analyses performed by Le Doux Co., Inc., Teaneck, N.J. Analytical methods: carbon - conductometric; oxygen - inert gas fusion; nitrogen - microkjeldahl; hydrogen - vacuum extraction; columbium - photo-colorimetric; others - spectrographic.

All analyses reported in parts per million unless indicated otherwise.

* Indicates that actual values are less than values shown, which are the lower limit of detection for the analytical method used.

TABLE 7
RELATIVE INTERSTITIAL LEVEL OF ELECTRODES, ELECTRODE STUBS,
AND INGOTS

	<u>ppm Carbon</u>	<u>ppm Oxygen</u>	<u>ppm Nitrogen</u>	<u>ppm Hydrogen</u>
06208-8	93	18	4	3.3
Stub	77	9	8	2.0
VA-68	44	9	9	8.3
09115-4	47	5	7	2.9
Stub	62	7	19	3.9
VA-83	123	8	13	3.7
W3-1-C	10	30	7	4.0
Stub	14	53	10	4.0
VA-87	51	25	12	1.8
11234-2	45	25	13	4.3
Stub	89	22	19	3.8
VA-88	226	15	20	2.1
11234-3	70	20	8	5.0
Stub	96	18	10	4.0
VA-91	157	28	19	1.8
WC-5	36	8	7	6.6
Stub	8	14	18	3.4
VA-86	6	21	6	1.2
W6-3-0	23	552	8	5.4
Stub	15	560	16	3.4
VA-90	21	31	18	0.5
W7-1-0	18	910	12	2.5
Stub		840	20	2.6
VA-92	25	12	12	2.4
09297-8	22	5	9	1.2
Stub	22	15	9	5.3
VA-78	10	17	22	1.1
09297-14	38	6	15	1.4
Stub	20	12	10	2.5
VA-79	18	9	14	0.8
09297-9	27	2	4	1.2
Stub	24	14	18	2.1
VA-80	9	20	10	0.9
09297-4	21	9	10	1.1
Stub	20	19	5	2.2
VA-81	10	18	26	1.5
09297-11	27	10	8	0.9
Stub	23	16	27	1.5
VA-82	8	19	28	2.3

TABLE 8

COMPARATIVE CARBON AND OXYGEN ANALYSES FOR W+O.6Cb SAMPLES

<u>Sample</u>	<u>ppm Carbon</u>	<u>ppm Oxygen</u>
09115-4	135(a), 27,47(b), 22(e)	12(a), 5(b), 36(d)
Stub	62(b)	7(b)
VA-83	123(b), 120(e)	8(b), 9(e)
W3-1-C	10(b), 50,80(d)	30(b), 53,60(d)
Stub	14(b), 37(e)	53(b), 64(d)
VA-87	51(b), 59(e)	25(b), 7(d)
11234-2	240(a), 45,49(b), 34(e)	4(a), 25(b), 19(d)
Stub	89(b), 210(e)	22(b), 22(d)
VA-88	226(b), 230,230(e)	15(b), 8(d)
11234-3	240(a), 70,125(b), 120(e)	4(a), 20(b), 40(d)
Stub	96(b), 54(e)	18(b), 47(d)
VA-91	157(b), 230,230(e)	28(b), 5,11(e)
WC-5	10,36(b), <30(c), 17(e)	6,8(b), 50(c), 13(d)
Stub	8(b), 32(e)	14(b), 24(d)
VA-86	6(b), 17(e)	21(b), 12(d)
W6-3-0	23(b), 29(d)	552(b), 500(d)
Stub	15(b), 17(e)	560(b), 480(d)
VA-90	21(b), 15(e)	31(b), 5(d)
W7-1-0	18(b)	910(b)
Stub	6(e)	840(b), 1052(d)
VA-92	25(b), 11(e)	12(b), 6(d)
09297-8	<10(a), 22(b), 14(e)	25(a), 5(b), 36(d)
Stub	22(b), 9(e)	15(b), 27(d)
VA-78	10(b), 22(e)	17(b), 7(d), 4,8(e)
09297-14	<10(a), 38(b), 24(e)	25(a), 6(b), 33(d)
Stub	20(b), 14(e)	12(b), 36(d)
VA-79	18(b), 15(e)	9(b), 11(d)
09297-9	<10(a), 27(b), 9(e)	25(a), 2(b), 27(d)
Stub	24(b), 5(e)	14(b), 33(d)
VA-80	9(b), 18(e)	20(b), 5,27(d), 154(e)
09297-4	<10(a), 21(b), 5(e)	25(a), 9(b), 23(d)
Stub	20(b), 14(e)	19(b), 58(d)
VA-81	10(b), 19(e)	18(b), 8,10(e)
09297-11	<10(a), 27(b), 9(e)	25(a), 10(b), 32(d)
Stub	23(b), 14(e)	16(b), 48(d)
VA-82	8(b), 34(e)	19(b), 9(d)

(a) General Electric Corp., Cleveland, Ohio

(b) Le Doux Co., Inc., Teaneck, N. J.

(c) Wah Chang Corp., Albany, Oregon

(d) Westinghouse Electric Corp., Blairsville, Pa.

(e) Westinghouse Research Laboratories, Churchill, Pa.

TABLE 9
HARDNESS OF W+0.6Cb INGOTS
(Average of 5 R_a Readings)

Ingot Number	Center		Mid Radius		Edge	
	As Cast	Heat Treated	As Cast	Heat Treated	As Cast	Heat Treated
*VA-68 top	70.4	----	70.2	----	69.4	----
VA-78 top	65.5	69.0	66.7	66.6	66.3	65.4
VA-78 bottom	68.1	69.2	66.1	68.2	62.9	----
VA-79 top	67.0	69.0	66.4	64.8	67.6	66.2
VA-79 bottom	----	69.6	67.0	67.0	64.8	----
VA-81 top	68.6	65.2	68.8	69.0	67.8	63.2
VA-81 bottom	68.6	67.6	66.6	67.0	65.0	63.6
VA-82 top	68.6	69.0	68.2	68.0	67.6	66.2
VA-82 bottom	68.2	67.4	68.4	67.0	65.8	66.2
*VA-83U top	----	69.8	----	68.8	----	67.0
*VA-83U bottom	----	69.8	----	69.2	----	64.2
*VA-83L top	68.2	----	69.0	----	65.6	----
*VA-83L bottom	69.8	----	66.4	----	66.4	----
VA-85 top	69.0	----	69.0	----	----	----
VA-85 bottom	68.6	----	67.0	----	----	----
VA-86 top	68.0	----	69.2	----	----	----
VA-86 bottom	69.4	----	68.4	----	----	----
*VA-87 top	69.4	----	69.0	----	----	----
*VA-87 bottom	68.2	----	68.8	----	----	----
*VA-88 top	70.4	----	70.0	----	----	----
*VA-88 bottom	69.4	----	68.8	----	----	----
VA-89 top	68.6	----	68.0	----	64.8	----
VA-89 bottom	69.0	----	68.2	----	62.0	----
VA-90 top	70.2	----	69.2	----	63.2	----
VA-90 bottom	68.8	----	68.6	----	58.4	----
*VA-91 top	69.6	----	69.8	----	66.2	----
*VA-91 bottom	70.4	----	69.6	----	66.0	----
VA-92 top	69.0	----	68.2	----	68.8	----
VA-92 bottom	68.8	----	68.6	----	66.4	----
Averages	68.8 (68.3)	68.6	68.3 (67.6)	67.6	65.5 (66.3)	65.3

Figures in () indicate average hardness of ingots up to VA-83 for comparison with heat-treated hardness.

*Indicates ingots that would not extrude.

TABLE 10
SUMMARY OF W+0.6 Cb EXTRUSION DATA

Extr. No.	Ingot No.	Billet Size (in.)	Billet Wt. (lb.)	Glass	Extr. Temp. (°F)	Ratio	Max. Force (tons)	Min. Force (tons)	Peak "K" Factor	Extr. Dia. (in.)	Remarks
896	VA-68	2.944 Ⓞ 3.625 L	16.9	7810	3800	6.2:1	740	640	-----	-----	Stuck
935	VA-78	2.942 Ⓞ 4.813 L	22.8	7810	3800	6.4:1	515	470	75,600	1.208	Exc. surface
936	VA-79	2.940 Ⓞ 4.938 L	22.1	7810	3800	8.3:1	590	560	76,000	1.065	Exc. surface
946	VA-81	2.940 Ⓞ 5.125 L	23.2	7810	3800	6.4:1	530	470	77,700	1.213	VG surface
947	VA-82	2.937 Ⓞ 5.063 L	23.3	7810	3800	6.4:1	495	470	72,600	1.212	Gd surface
948	VA-83U	2.941 Ⓞ 5.000 L	23.2	7810	3800	6.4:1	720	---	-----	-----	Stuck
951	VA-83L	2.941 Ⓞ 5.000 L	23.1	7900	4200	3.0:1	620	---	-----	-----	Stuck
955	VA-85	2.940 Ⓞ 5.031 L	23.2	7810	3800	6.4:1	570	520	83,500	1.208	Gd surface
956	VA-86	2.937 Ⓞ 5.000 L	23.0	7810	3800	6.4:1	500	430	73,200	1.215	Gd surface
957	VA-87	2.942 Ⓞ 5.000 L	23.1	7810	3800	6.4:1	630	---	-----	-----	Stuck
958	VA-88	2.944 Ⓞ 5.031 L	23.4	7810	3800	6.4:1	590	---	-----	-----	Stuck
964	VA-89	2.938 Ⓞ 5.031 L	23.2	7810	3800	6.3:1	550	480	81,300	1.220	Fr surface
965	VA-90	2.945 Ⓞ 5.031 L	23.3	7810	3800	6.2:1	No Reading	---	-----	1.228	38 sec transf Fr surface
966	VA-91	2.940 Ⓞ 4.983 L	23.0	7810	3800	6.4:1	640	---	-----	-----	Stuck
974	VA-92	2.938 Ⓞ 5.031 L	23.2	7810	3800	6.3:1	570	400	84,200	1.220	Pr surface

Billet end shape, 0.25" x 45° bevel
Nose block, 1018 steel coated with 8871 glass and heated to 1600°F
Follower block, machined graphite

TABLE 11
 HARDNESS OF W+0.6Cb EXTRUSIONS
 (Average of 3 R_a Readings)

<u>Extrusion (Ingot) Number</u>	<u>Nose</u>		<u>Center</u>		<u>Tail</u>	
	<u>Center</u>	<u>Edge</u>	<u>Center</u>	<u>Edge</u>	<u>Center</u>	<u>Edge</u>
935 (VA-78)	70.7	71.3	70.0	69.7	73.0	73.0
936 (VA-79)	69.0	68.7	70.3	69.7	72.0	72.7
946 (VA-81)	71.0	73.0	70.7	71.7	72.3	72.7
947 (VA-82)	70.3	71.3	68.7	69.7	72.0	72.6
955 (VA-85)	69.3	72.0	69.3	69.0	72.7	73.3
956 (VA-86)	69.3	69.3	69.7	69.3	71.0	72.0
964 (VA-89)	72.3	73.0	72.0	71.0	73.3	72.3
965 (VA-90)	73.6	73.0	72.6	73.0	73.0	72.6
974 (VA-92)	71.0	72.3	69.7	70.0	73.0	72.7
Averages	70.7	71.5	70.3	70.3	72.5	72.6

TABLE 12

TENSILE DATA ON SWAGED W+0.6Cb ALLOY
(Tested in Vacuum at 3000°F)

Ingot Number	VA-78	VA-79	VA-81	VA-82	VA-85	VA-89	VA-90
Electrode Additions	none	none	0.06%Zr	0.04%Ti	0.12%Zr	0.12%Zr	0.12%Zr 500 ppm O
Extrusion Number	935	936	946	947	955	964	965
Stress at 0.2% Y.P. (psi)	41,400	43,500	44,400	37,000	47,700	49,000	37,200
Stress at 0.5% Y.P. (psi)	42,500	44,800	45,700	38,800	50,000	50,700	38,300
Ultimate Stress (psi)	42,740	45,000	46,470	38,960	54,250	51,940	38,760
Uniform Strain (%)	0.65	0.70	0.80	0.40	2.4	1.0	0.6
Fracture Stress (psi)	10,940	11,470	21,630	5,420	25,430	22,950	13,470
Fracture Strain (%)	12.4	13.3	10.3	14.1	14.1	11.8	10.9
Reduction of Area (%)	84.2	89.1	75.6	93.4	75.7	75.5	77.9
Elongation (%)	13.3	14.0	10.7	14.7	13.3	13.3	11.3

Specimens were machined from .625 inch stock which was reduced 56 percent after annealing.

Specimens were maintained for 15 minutes at temperature before stress was applied.
Strain Rate: 300% per hour.
Maximum pressure during heating: 0.17 microns.
Average pressure during test: 0.02 microns.

TABLE 13
SUMMARY OF VACUUM ARC MELTING FOR SUPPORT PROGRAM

<u>Heat No.</u>	<u>VA-69</u>	<u>VA-70</u>	<u>VA-71</u>	<u>VA-72</u>	<u>VA-73</u>	<u>VA-74</u>	<u>VA-75</u>	<u>VA-76</u>	<u>VA-77</u>	<u>VA-84</u>
<u>Alloy</u>	92-6-2	92-6-2	92-6-2	92-6-2	92-6-2	92-6-2	92-6-2	92-6-2	92-6-2	92-6-2
<u>Electrode</u>										
Density, %	92.5	92.0	92.5	92.3	92.1	92.2	92.2	92.4	100	92.1
Length, in.	52	52	50	51	55.5	56	53.5	54.5	39	53.4
Weight, lb.	54.6	54.2	51.0	52.8	58.2	59.0	53.8	56.8	5.5	52.5
Camber, in.	1/8	1/8	3/32	1/16	1/16	1/16	1/8	1/16	0	1/16
Melting Amperage	5400	5600	5800	5800	5800	5800	5800	5800	1600	5800
Arc Voltage	28	28	28	30	28	28	28	28	28	28
Stirring Amperage	1/2	1	1/2	2	2	2	3	3	3	2
Melting KW	152	157	163	174	163	163	163	163	45	163
Melting Rate, lb/min.	1.34	1.53	1.73	1.79	1.77	1.90	1.81	.78	1.4	1.68
Average Melt Pressure (u)	.09	.05	.08	.05	.06	.04	.05	.06	.02	.04
Melting Time, min.	40	38.3	28.8	33.6	33.3	30.3	33.0	34.6	3.3	34.3
Ingot Weight, lb.	62.3	61.8	58.4	59.5	60.8	63.2	61.0	62.4	5.9	61.7

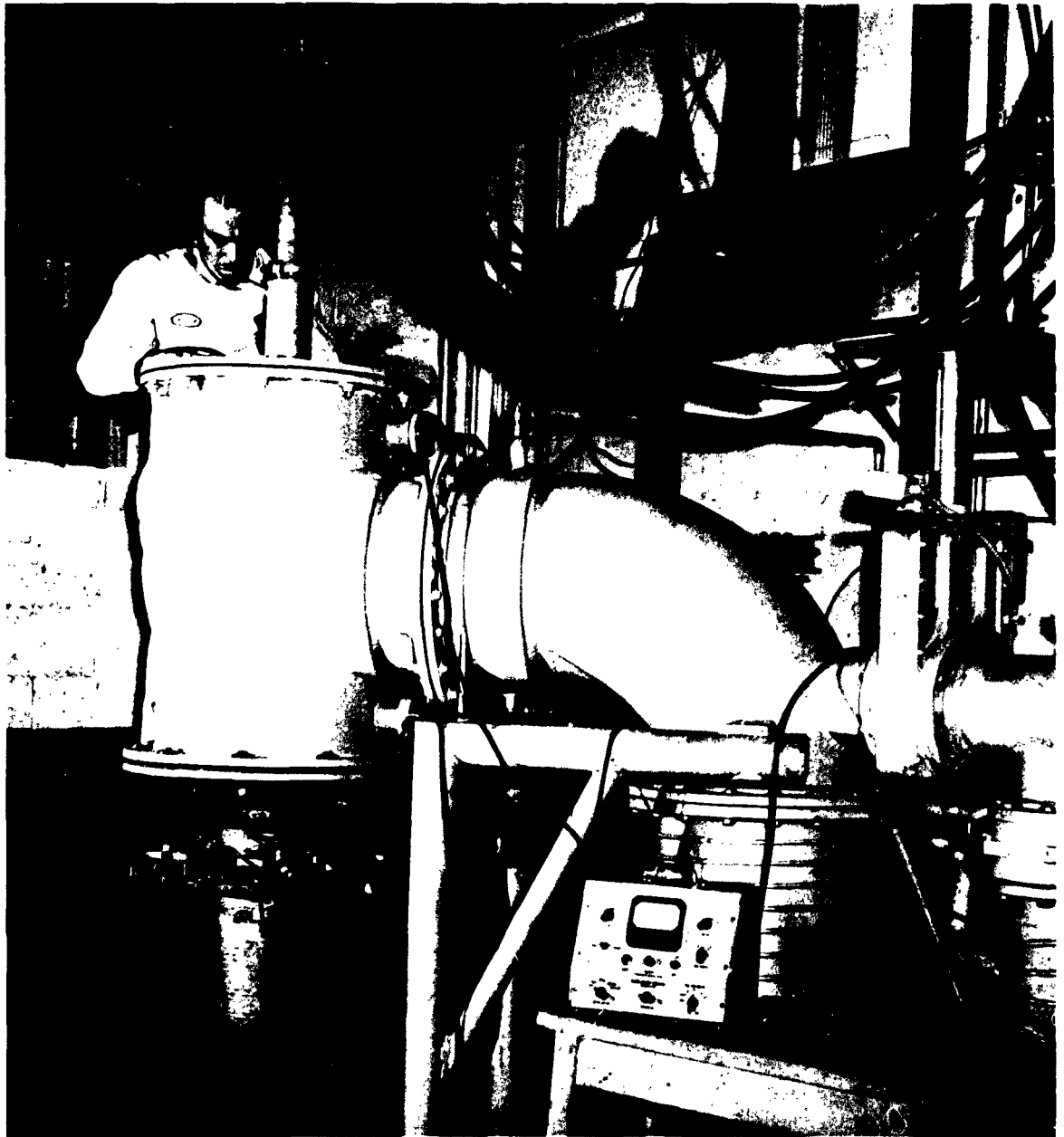


Figure 1 - Vacuum Arc Melting Facility at ASD. Pump Capacity Permits Melting of Refractory Alloys at Pressures Below 0.1 Micron. Silicon Rectifiers Supply up to 7500 Amperes.

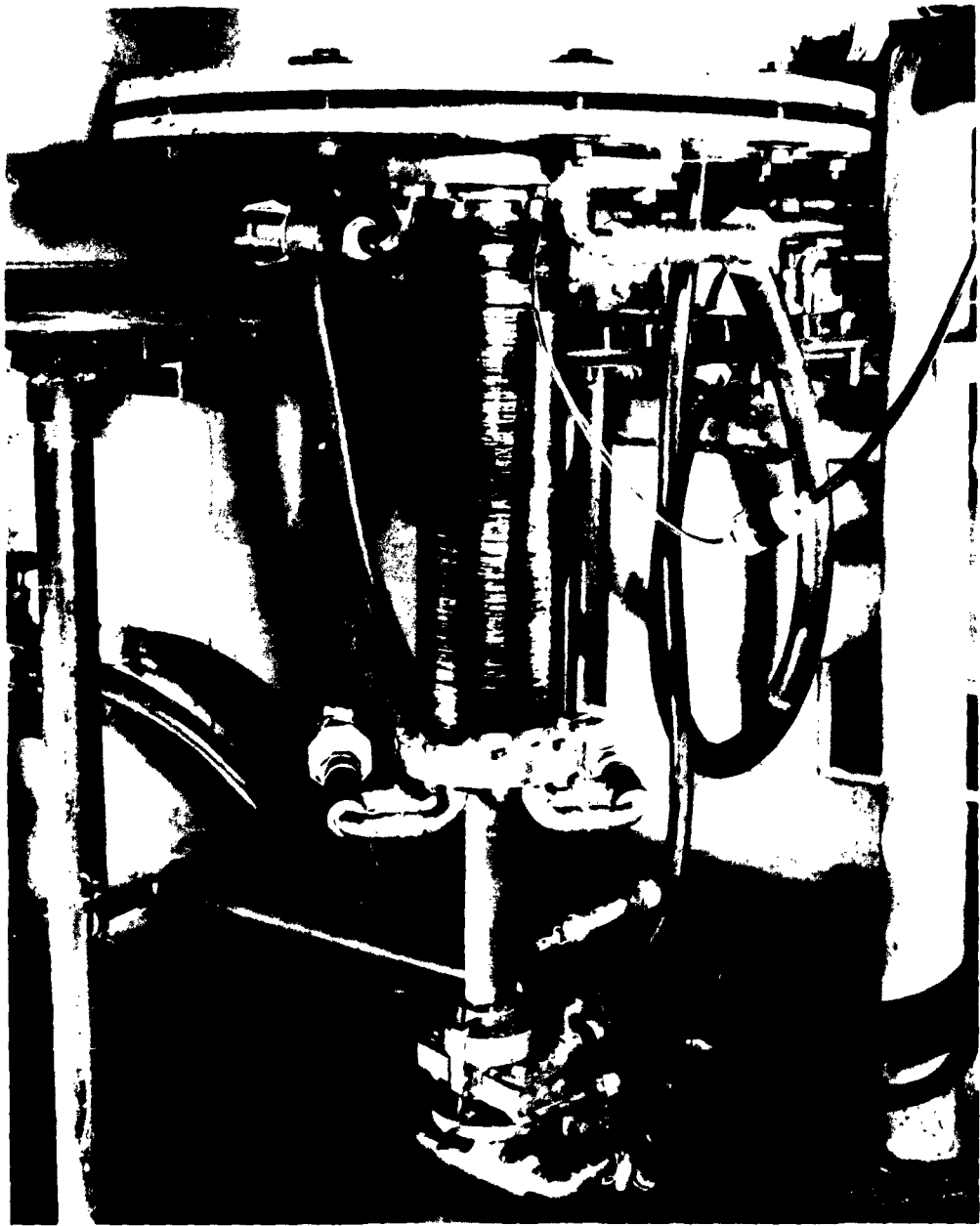


Figure 2 - Redesigned Water Jacket Assembly Mounted on Furnace. Annular Space for Water Flow Around Mold is 1/8 Inch. Current is Conducted From Ingot Through Mold Bottom.

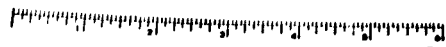
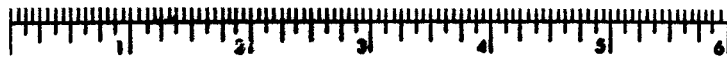


Figure 3 - Examples of Threaded Electrode Sections. Sources of Electrode Bars Are (L to R): General Electric, Wah Chang, Westinghouse. Columbian Wire Addition Is Shown in Left Electrode, Others Are Tungsten + 0.6% Columbian Blend.



VA-66

VA-67

Figure 4 - Ingot Sections of W+0.6Cb Heats VA-66 and VA-67.

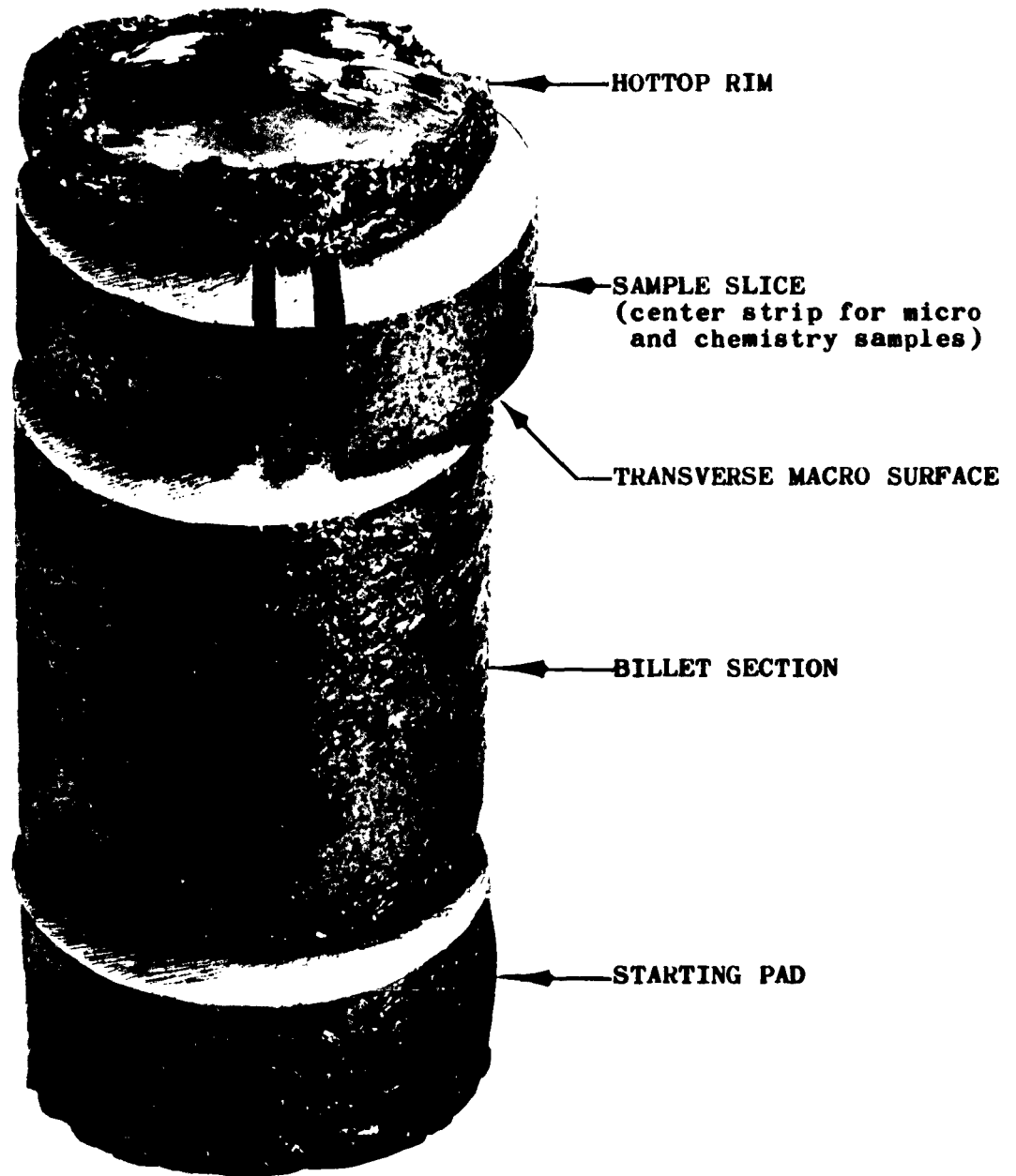


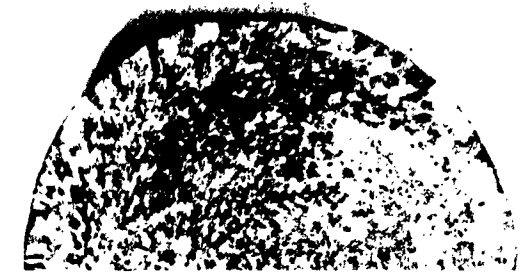
Figure 5 - Method of Cutting W+0.6Cb Ingots for Samples and Billet.



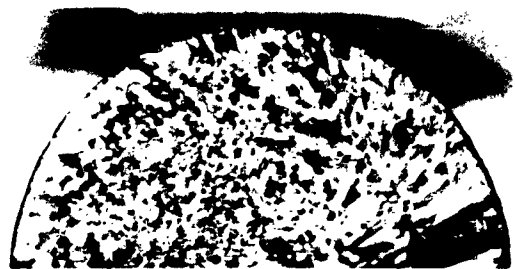
Figure 6 - W+0.6Cb Ingot VA-83. The Length of This Ingot was Sufficient to Produce Two 5-Inch Extrusion Billets. Ingot Surface is Considered Excellent.



VA-83



VA-88



VA-91



VA-87

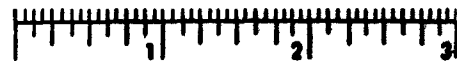
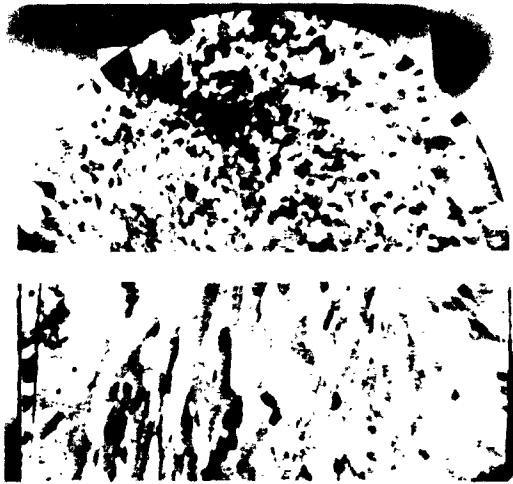
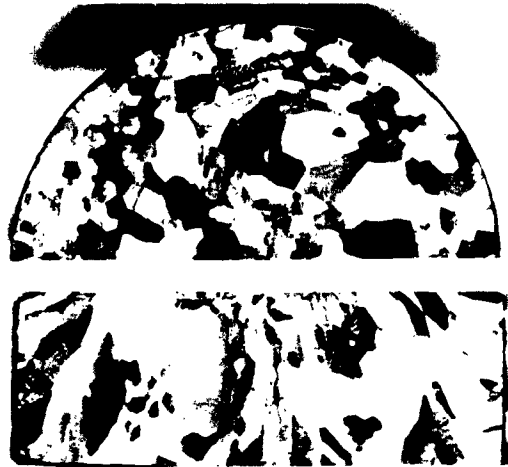


Figure 7 - Macrostructures of W+0.6Cb Ingots VA-83, VA-87, VA-88, and VA-91. All Four Ingots Contain an Excess of Carbon.



VA-86



VA-92



VA-90

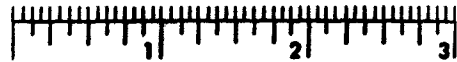
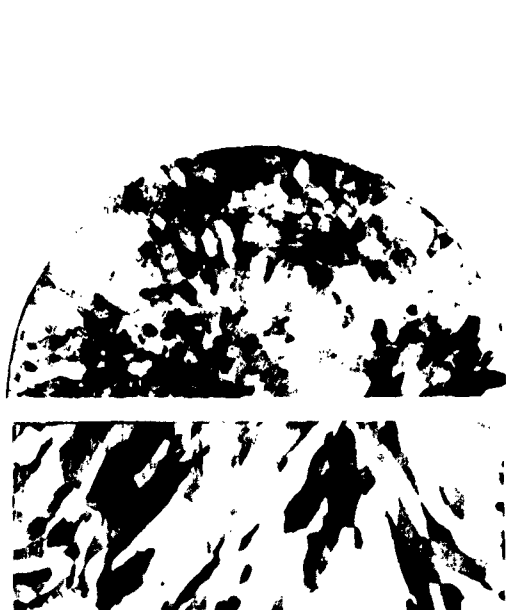
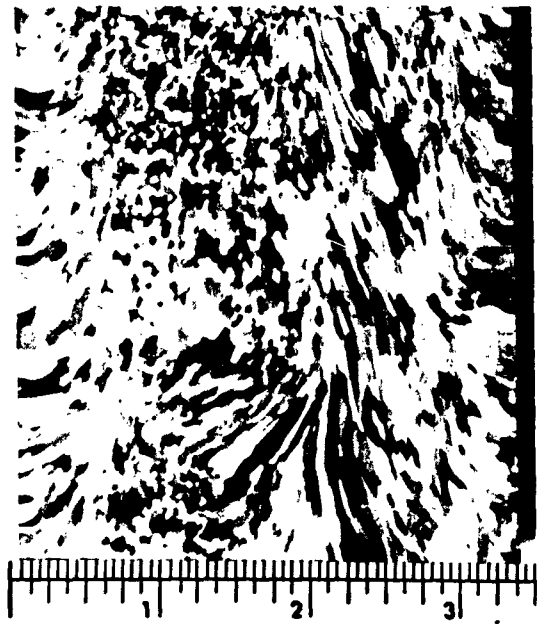
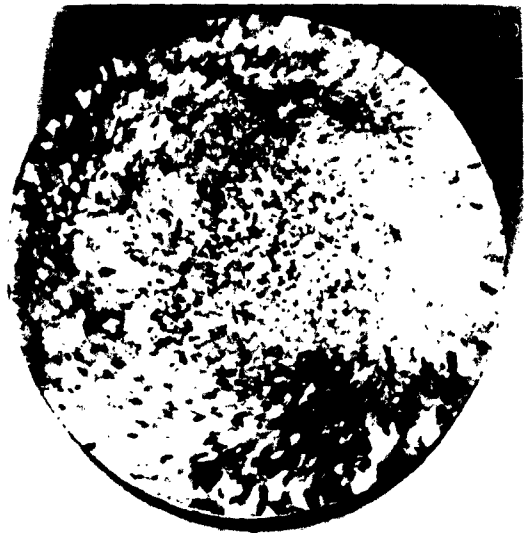


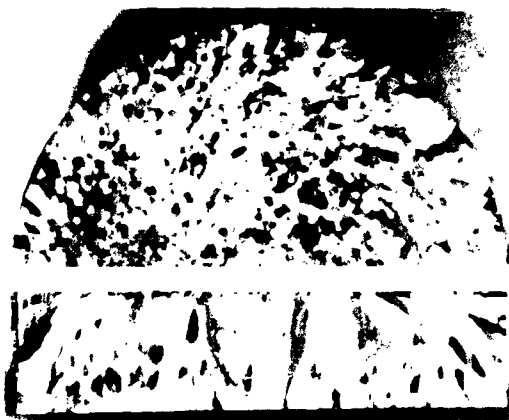
Figure 8 - Macrostructures of W+0.6Cb Ingots VA-86, VA-90, and VA-92. Electrodes Contained an Excess of Oxygen.



VA-78, 5800 Amperes



VA-80, 7200 Amperes



VA-79, 6500 Amperes

Figure 9 - Macrostructures of W+0.6Cb ingots VA-78, VA-79, and VA-80. Ingots Were Melted to Determine Effect of Power Input on Electrode Consumption and Ingot Structure.

MELTING RATE vs. INPUT FOR W+0.6Cb ALLOY

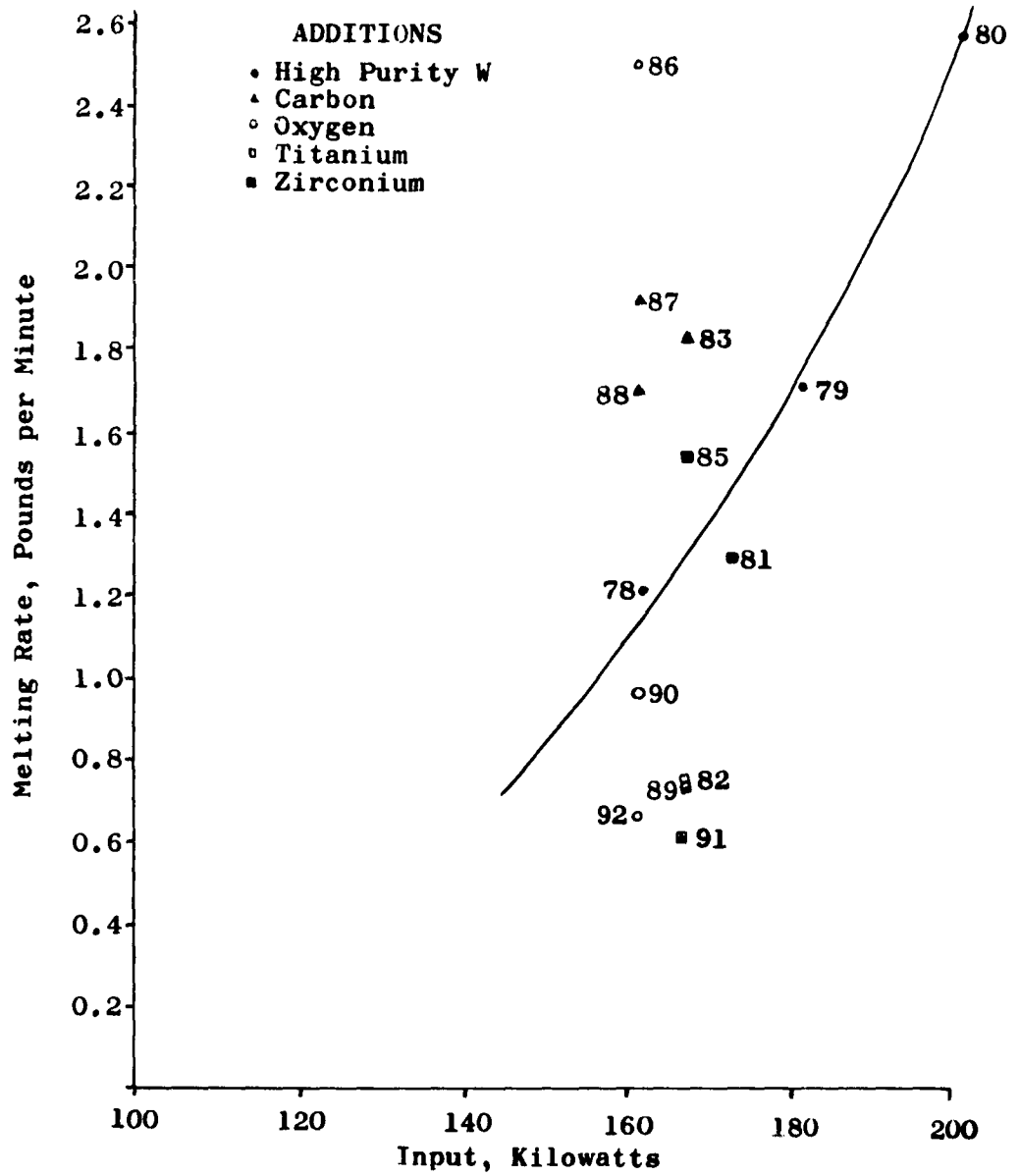


Figure 10

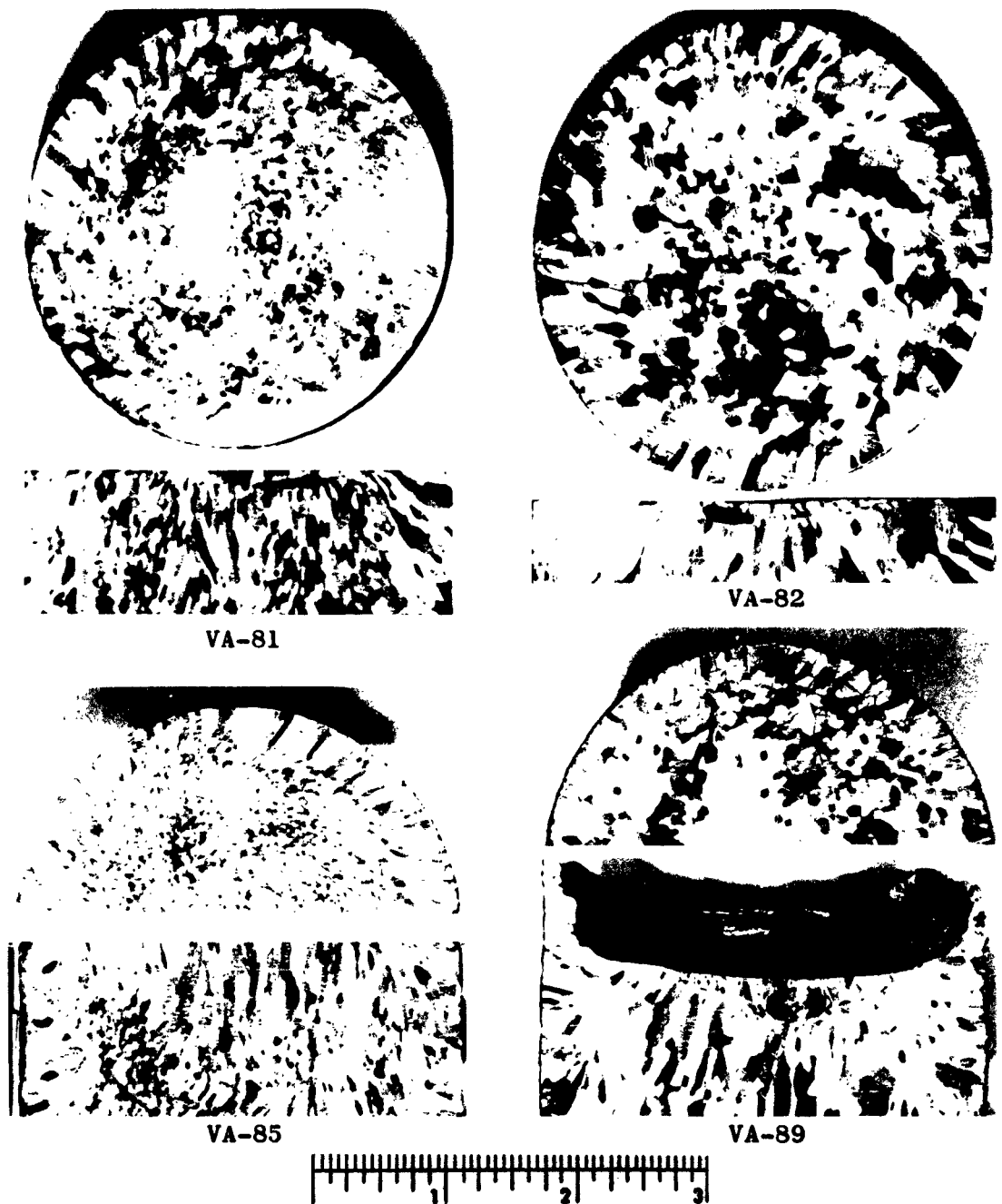
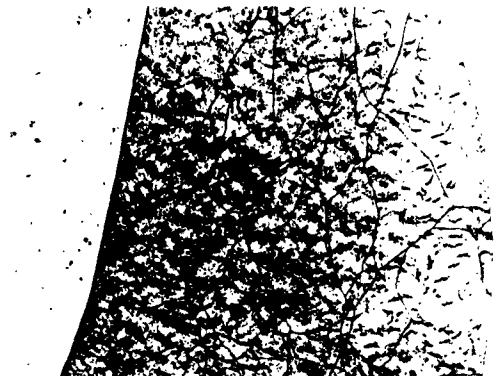


Figure 11 - Macrostructures of W+0.6Cb Ingots VA-81, VA-85, VA-82, VA-89. Electrodes Contained Zirconium and Titanium as Follows: VA-81, 0.06% Zr; VA-85, 0.12% Zr; VA-82, 0.04% Ti; VA-89, 0.04% Ti + 0.12% Zr.



VA-66, Mechanical Polish(100X)



VA-67, Mechanical Polish(100X)



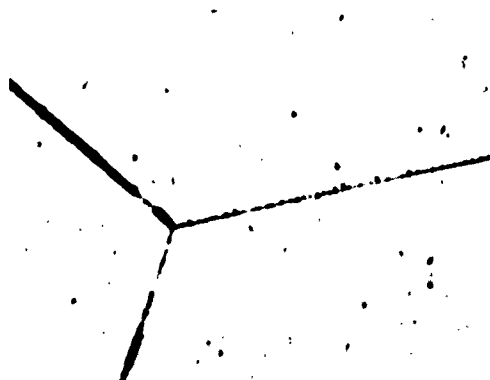
VA-66, Mechanical Polish(1000X)



VA-67, Electro-polished(1000X)



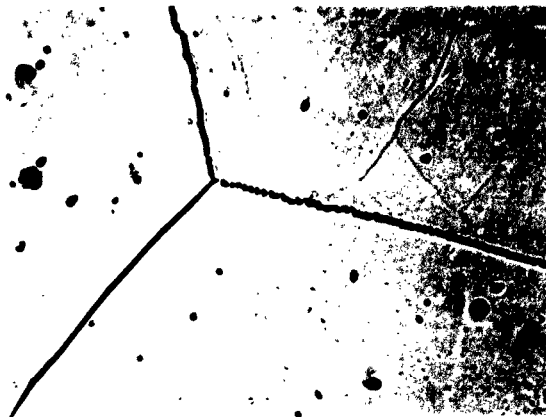
VA-66, Electro-polished(1000X)



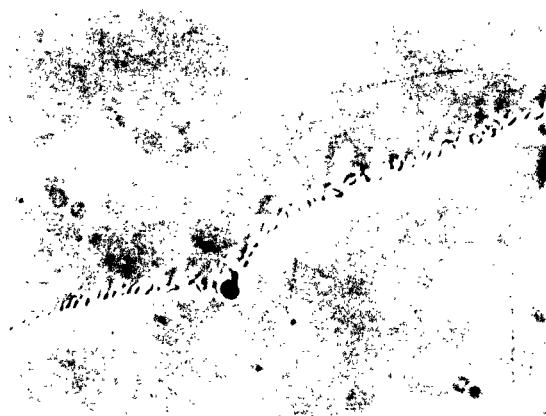
VA-67, Mechanical Polish(1000X)

Figure 12 - Microstructures of $\gamma+0.6\text{Cb}$ Ingots VA-66 and VA-67. Grain Boundary Deposits Are Evident at High Magnification.

Murakami's Etch



250X

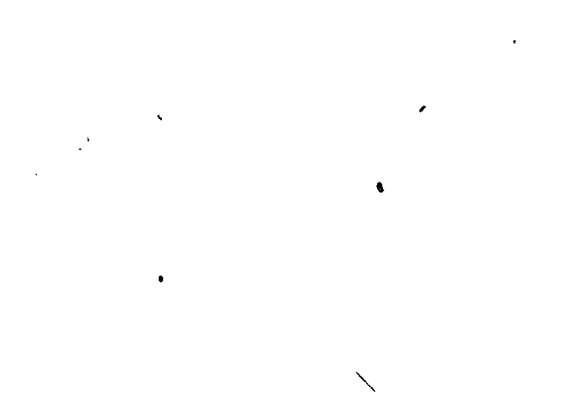


2000X



2000X

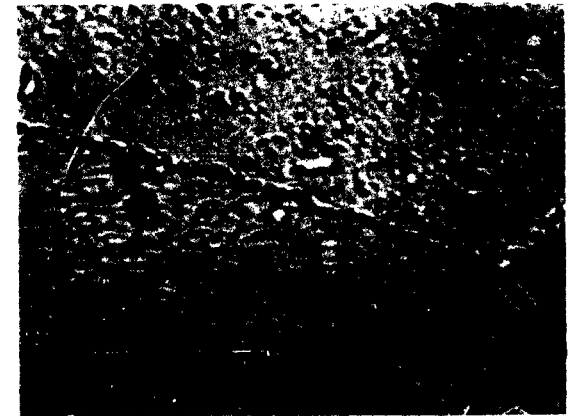
VA-83



250X



2000X



2000X

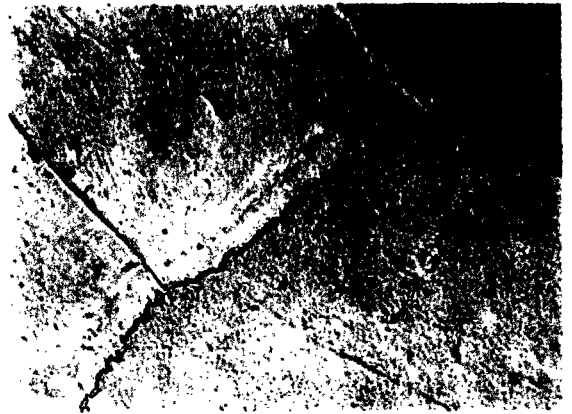
VA-87

Figure 13 - Microstructures of W+0.6Cb Ingots VA-83 and VA-87.
Grain Boundary Deposits Are Carbides.

Electrolytic Polish - Murakami's Etch



250X



250X



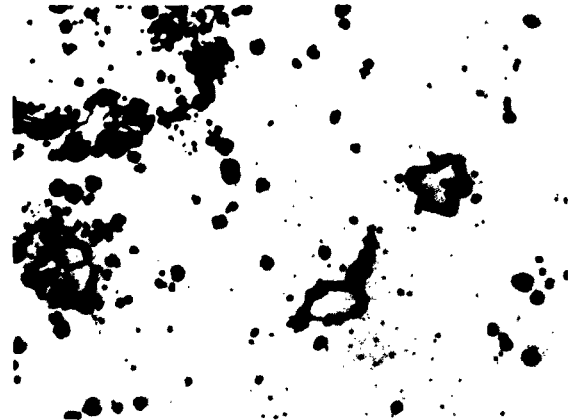
2000X



2000X



2000X



2000X

VA-88, High Carbon Electrode

VA-91, High Carbon + Titanium

Figure 14 - Microstructures of W+0.6Cb Ingots VA-88 and VA-91.

Electrolytic Polish - Murakami's Etch

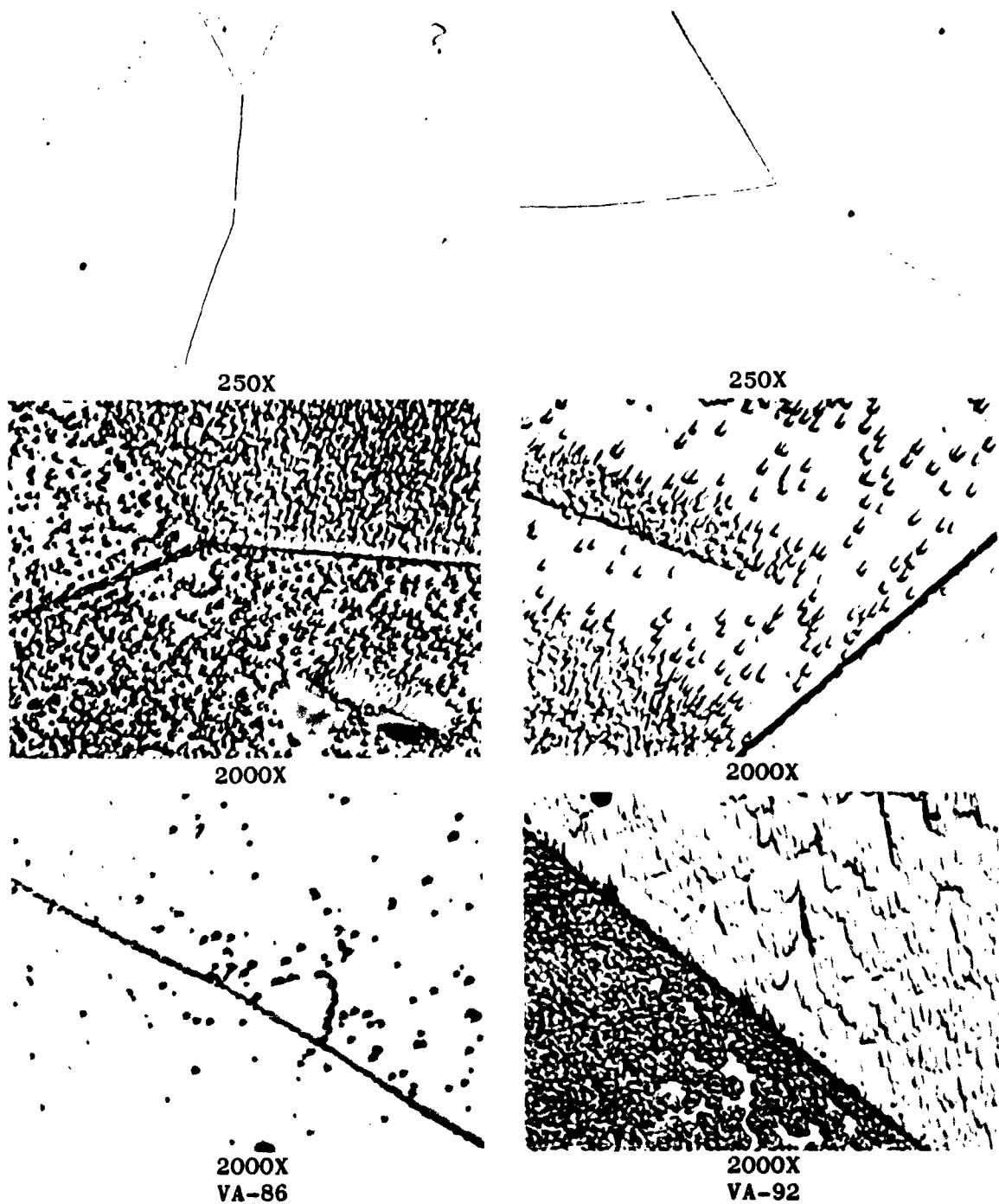
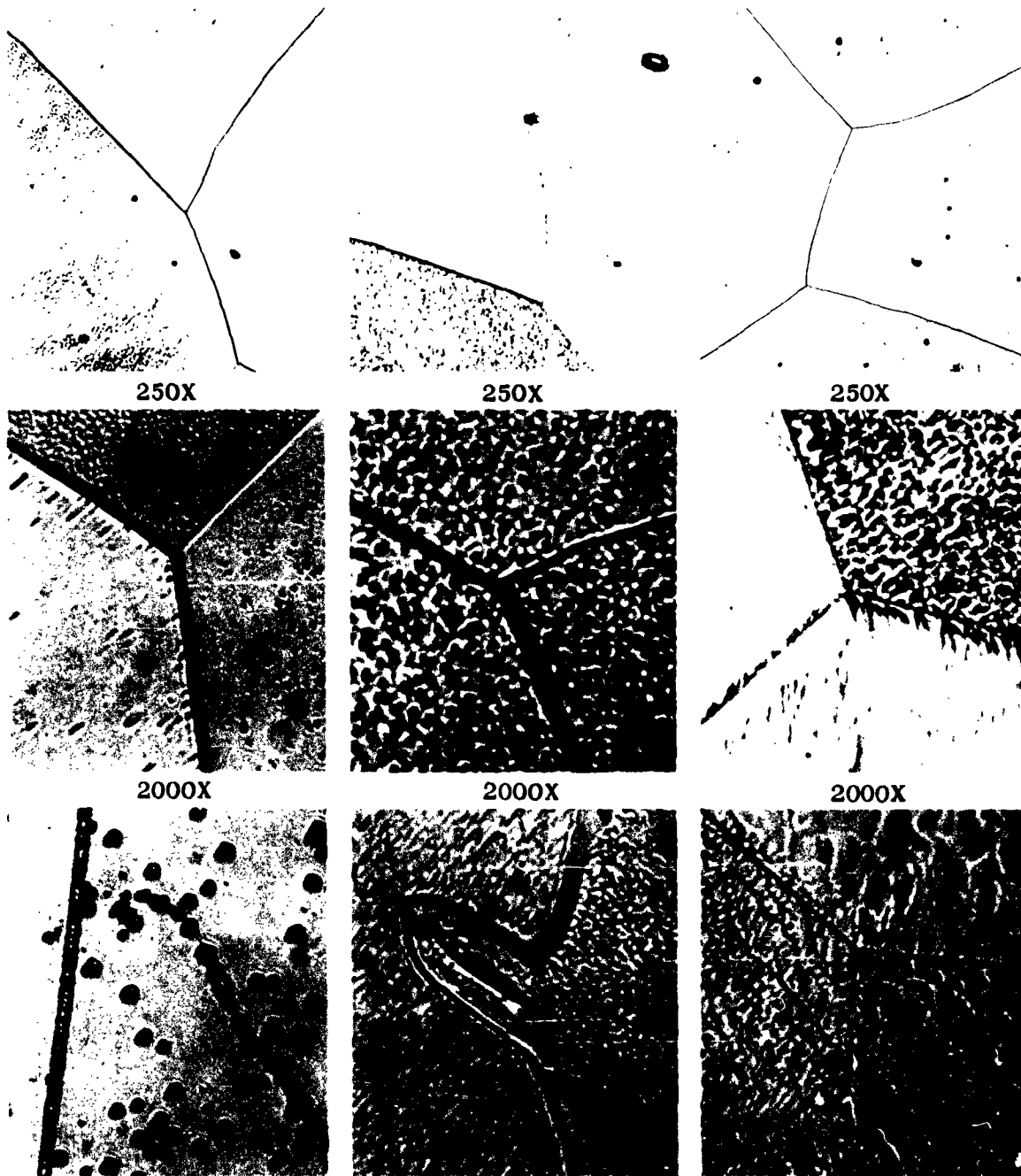
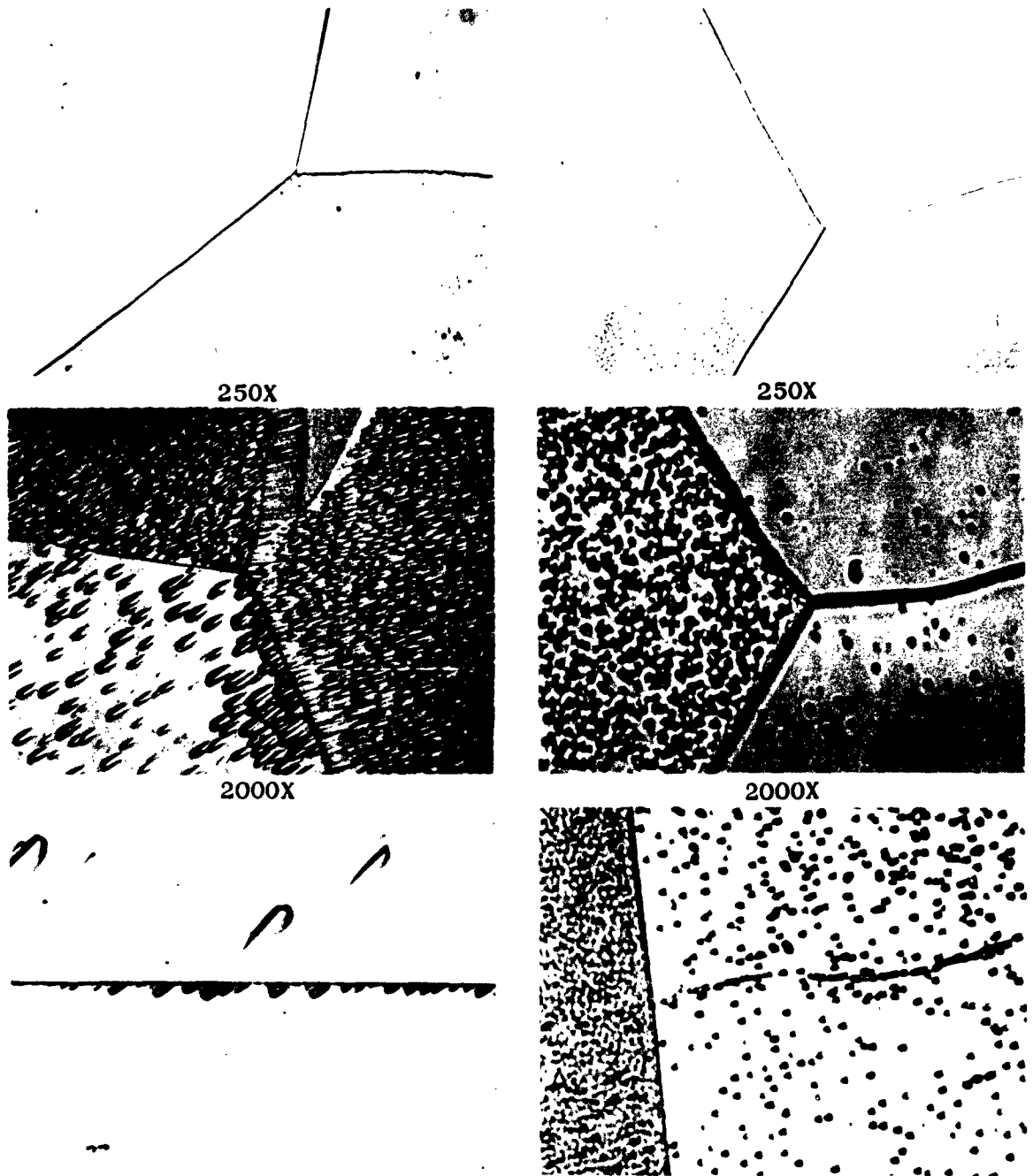


Figure 15 - Microstructures of W+0.6Cb Ingots VA-86 and VA-92. Electrodes Contained An Excess of Oxygen. Dark Region at Boundary Is Shadow, Not Deposit. Electrolytic Polish - Murakami's Etch



2000X VA-78, 5800 Amperes 2000X VA-79, 6500 Amperes 2000X VA-80, 7200 Amperes
 Figure 16 - Microstructures of W+0.6Cb Ingots VA-78, VA-79, and VA-80. Ingots Were Melted to Show Effect of Electrode Consumption Rate on Properties.

Electrolytic Polish - Murakami's Etch



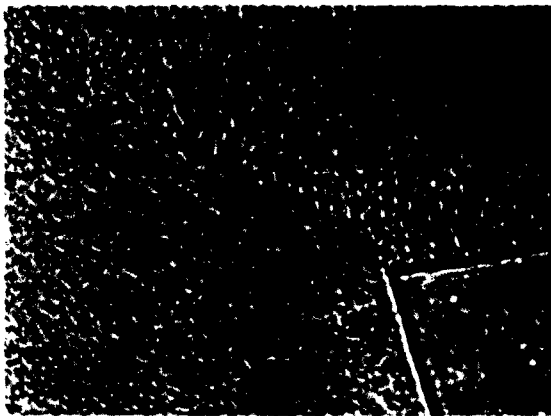
2000X VA-81, 0.06% Zr
 2000X VA-85, 0.12% Zr
 Figure 17 - Microstructures of W+0.6Cb Ingots VA-81 and VA-85.
 Electrodes Contained Minor Zirconium Additions.
 Electrolytic Polish - Murakami's Etch



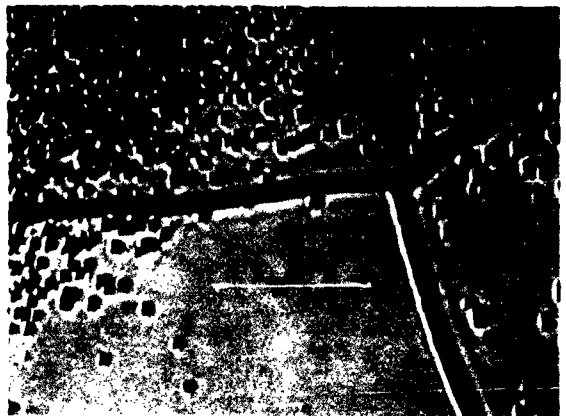
250X



250X



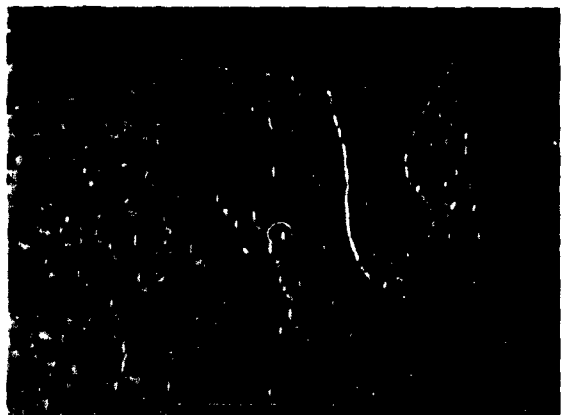
2000X



2000X

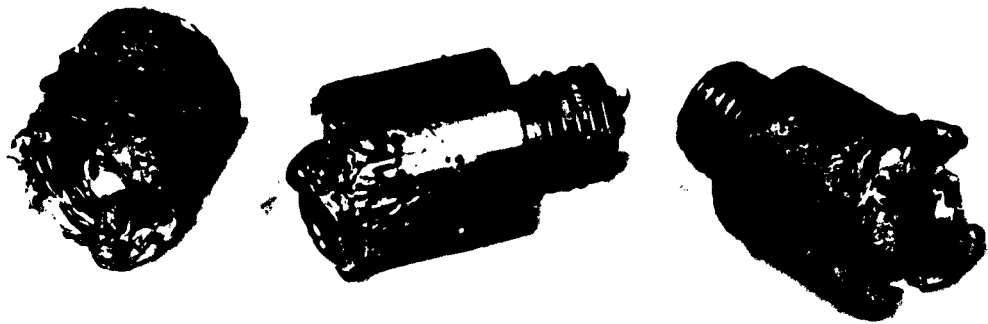


2000X



2000X

VA-82, 0.04% Ti
VA-89, 0.04% Ti + 0.12% Zr
Figure 18 - Microstructures of W+0.6Cb Ingots VA-82 and VA-89.
Electrodes Contained Titanium and Zirconium.
Electrolytic Polish - Murakami's Etch

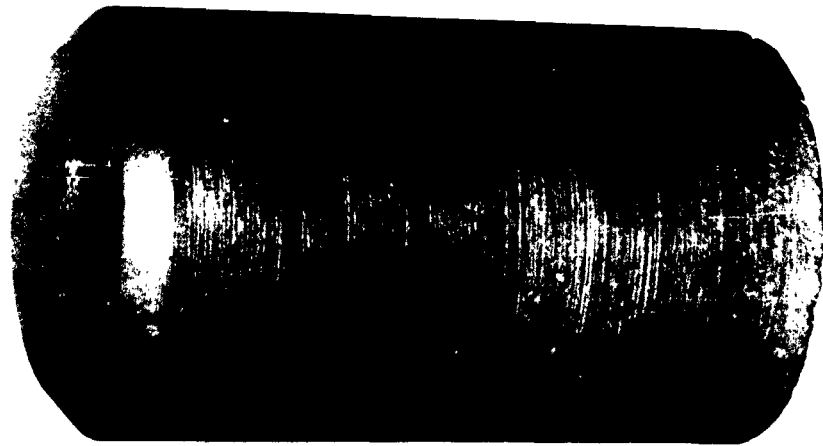


W7-1-0
(VA-92)

09297-12
(VA-89)

11234-3
(VA-91)

Figure 19 - Electrode Stubs Before Removal of Chemistry Samples.



VA-83L



VA-83U



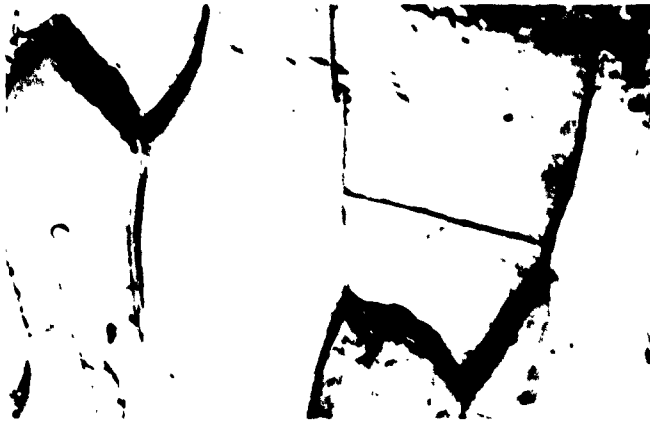
VA-90

1 2 3 4 5 6

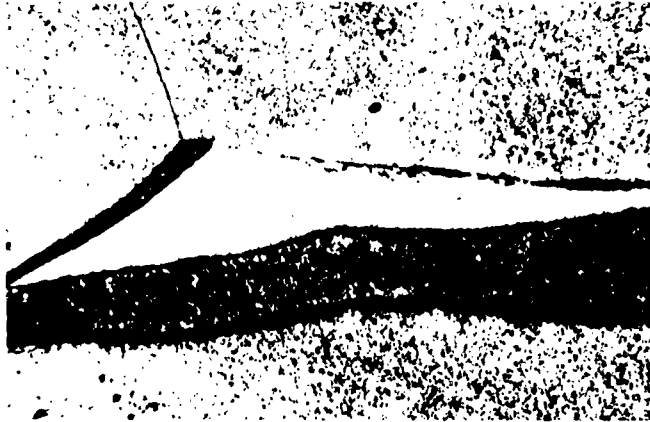
Figure 20 - Machined Billet and Unextruded Billet from Ingot VA-83 (High Carbon) and Machined Billet from Ingot VA-90 (High Oxygen).



Figure 21 - Extrusions of W+0.6Cb Alloy
63



Over-Etched Specimen,
Showing Deposit Extending
Above Sample Surface
(Approx. 30X)



Intergranular Deposit at
150X. Spheroidal Particles
Indicate Material was
Liquid.



Fracture Surface (250X)

Figure 22 - Intergranular Deposit in Unextruded Billet From
Ingot VA-68.



Figure 23 - Closeup of Extrusion Surfaces. Bars were Sandblasted to Remove Lubricant and Sil-O-Cel.



956



965



974



Figure 24 - Closeup of Extrusion Surfaces Showing Defects Peculiar to Material Originating from High Oxygen Electrodes.

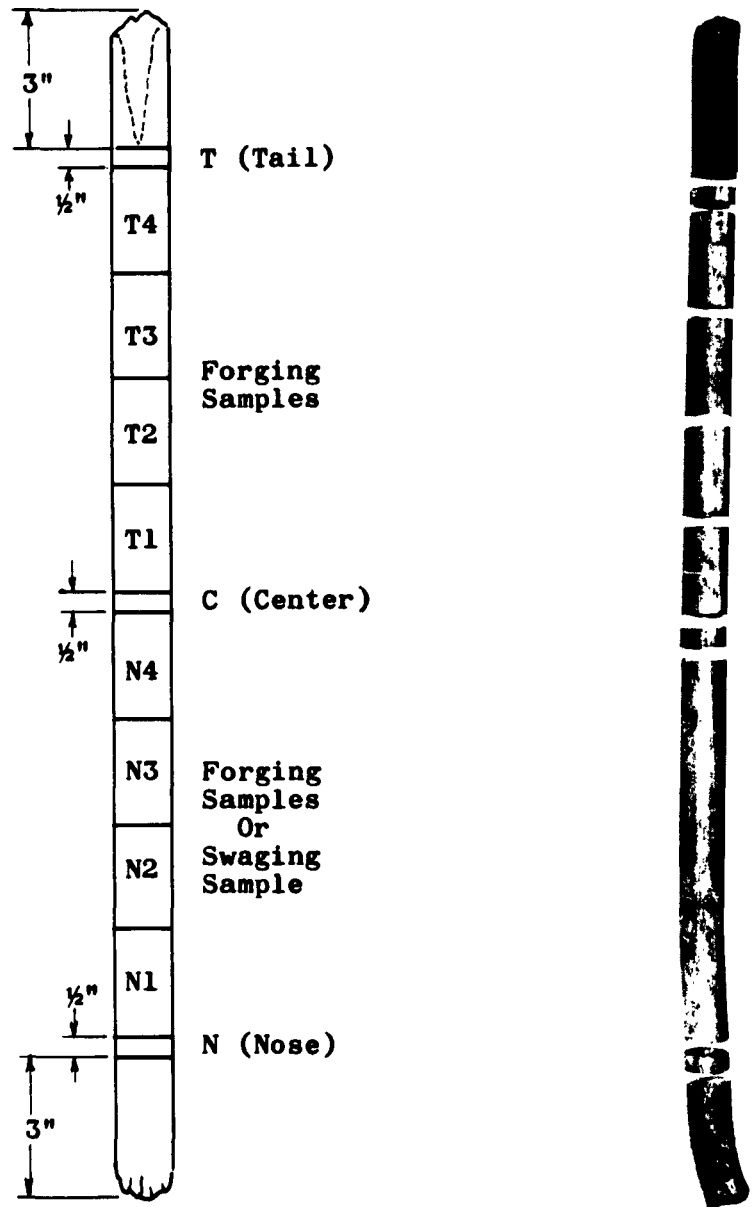
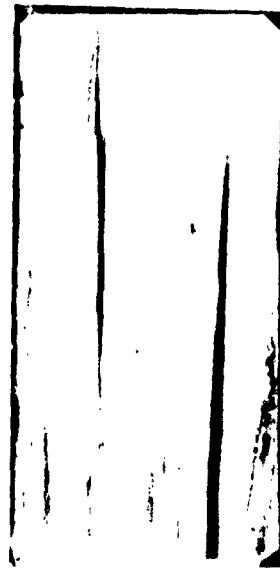
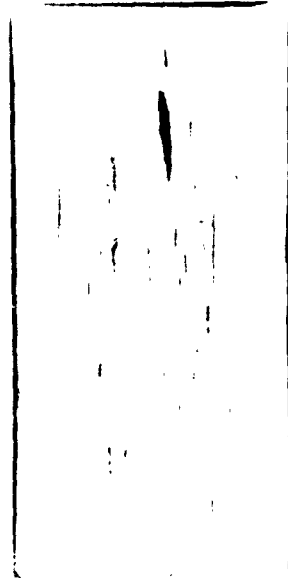
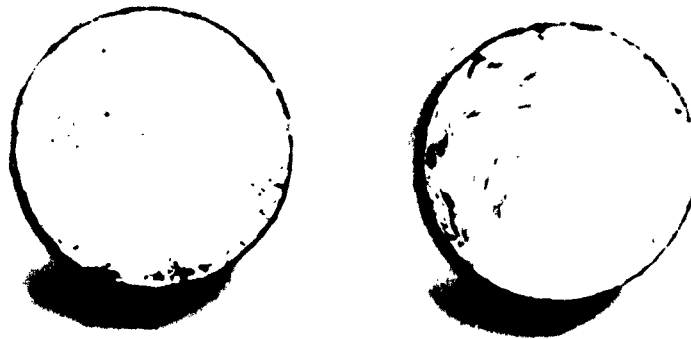


Figure 25 - Extrusion Sample Identification Diagram



956T1

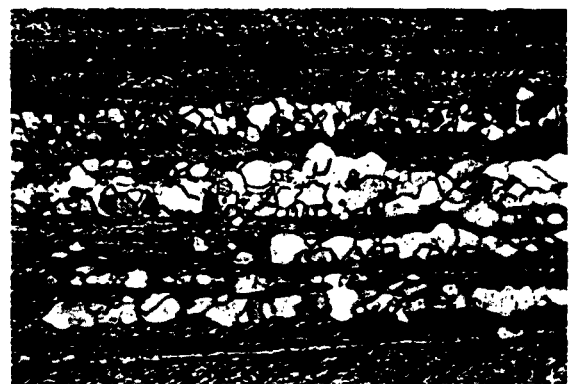
974N4



Figure 26 - Transverse and Longitudinal Macrosections of Extrusions 956 and 974. Difference in Structure of Extrusions May Be Compared to Difference in Structure of Ingots from Which These Extrusions Originated by Referring to Figure 8, Ingots VA-86 and VA-92.



Nose



Center



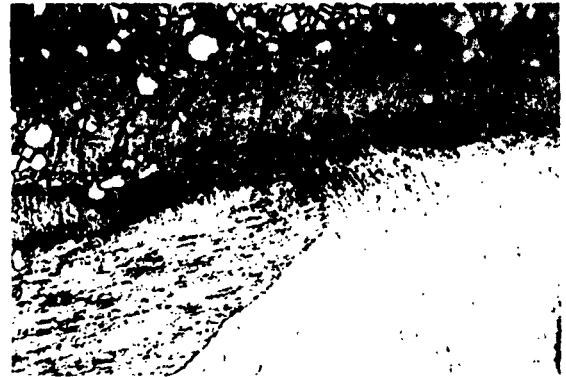
935 (VA-78) 100X
6.4:1

Tail

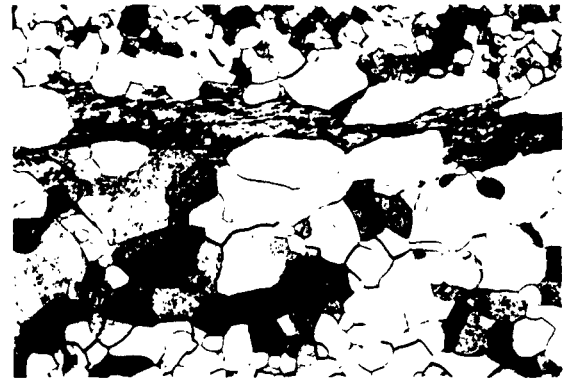
936 (VA-79) 100X
8.3:1

Figure 27 - Microstructures from Nose, Center, and Tail Samples of Extrusions 935 and 936.

Electrolytic Polish - Murakami's Etch



Nose



Center



946 (VA-81) 100X

Tail

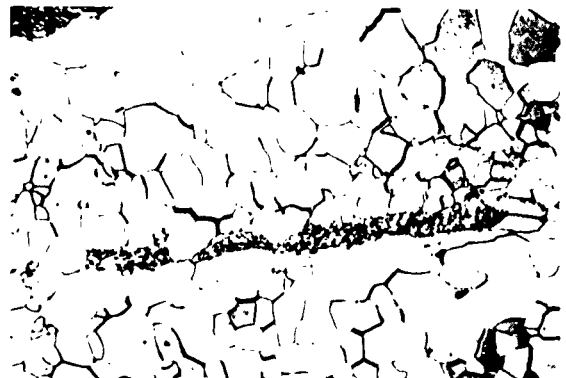
947 (VA-82) 100X

Figure 28 - Microstructures from Nose, Center, and Tail Samples of Extrusions 946 and 947. Notice Slightly Deformed Grains of Original As-Cast Structure in Nose Sample of 947.

Electrolytic Polish - Murakami's Etch



Nose



Center



955 (VA-85) 100X

Tail

956 (VA-86) 100X

Figure 29 - Microstructures from Nose, Center, and Tail Samples of Extrusions 955 and 956.

Electrolytic Polish - Murakami's Etch



Nose



Center



964 (VA-89) 100X

Tail

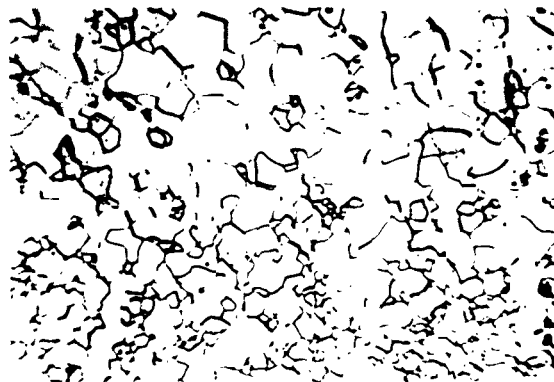
965 (VA-90) 100X

Figure 30 - Microstructures from Nose, Center, and Tail Samples of Extrusions 964 and 965. No Recrystallization Occurred in 965 due to Billet Heat Loss Prior to Extrusion.

Electrolytic Polish - Murakami's Etch



Nose



Center



Tail

974 (VA-92) 100X

Figure 31 - Microstructures from Nose, Center, and Tail Samples of Extrusion 974.

Electrolytic Polish - Murakami's Etch



935

946

947

Figure 32 - Extrusion Forging Samples, Machined Forging Samples, and Forged Samples of W+0.6Cb Alloy.

1/T vs. TIME FOR RECRYSTALLIZATION OF W+0.6Cb
 (Samples Reduced 55% by Forging)

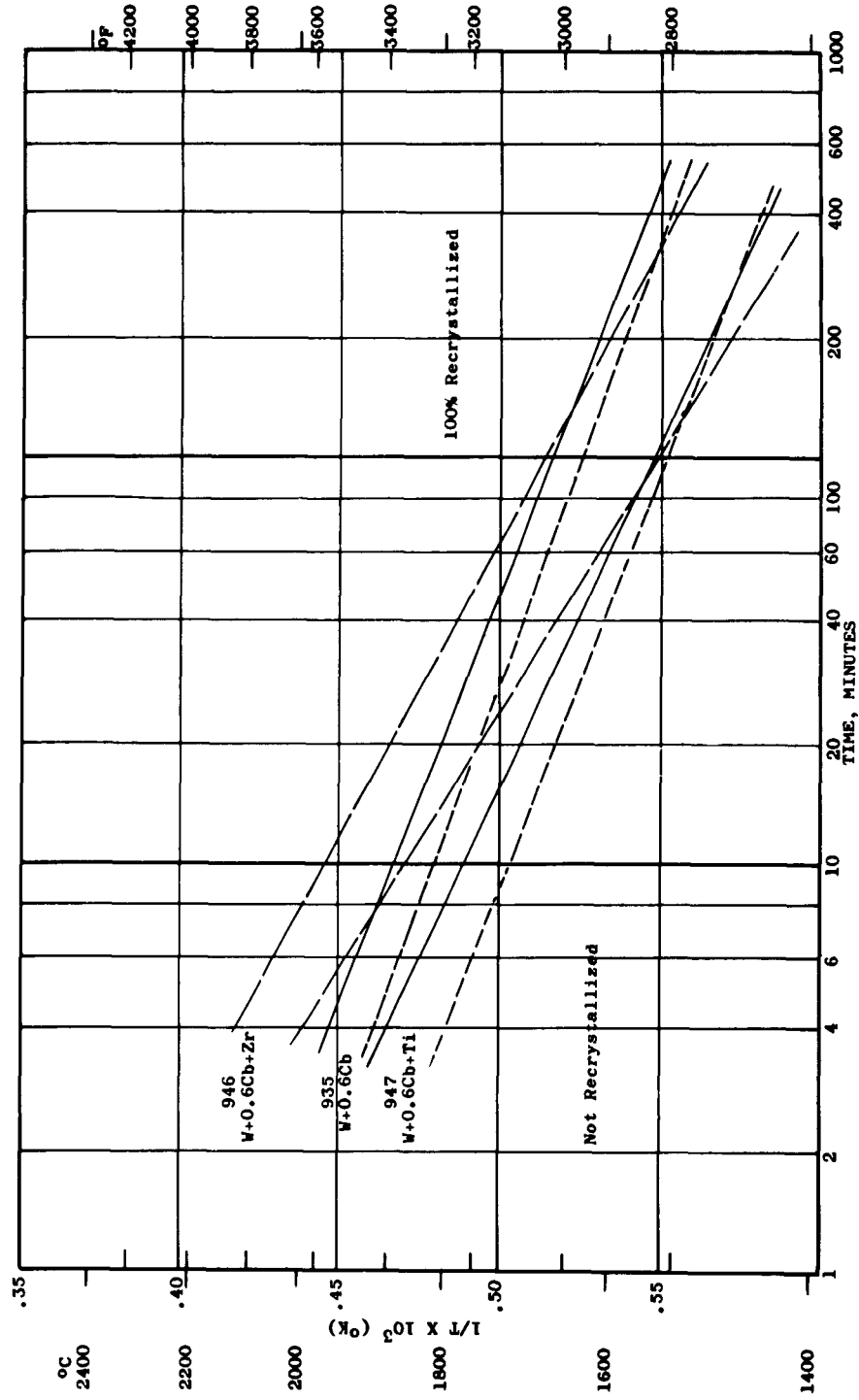
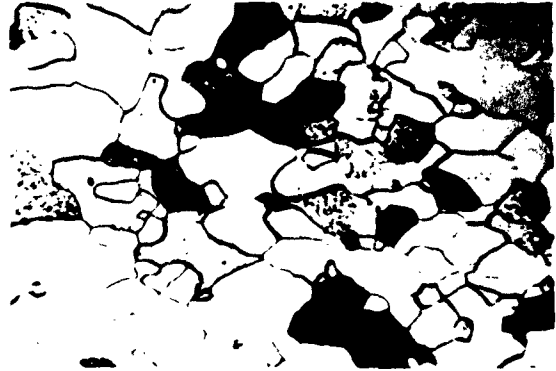


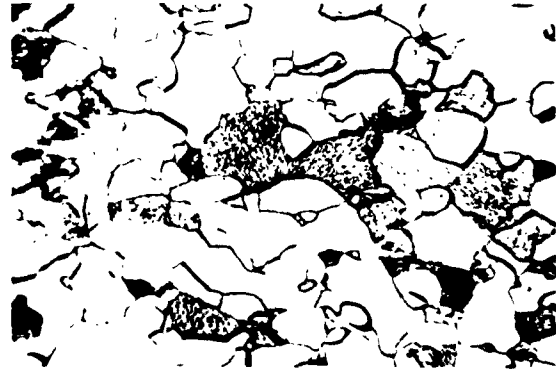
Figure 33



935 (VA-78), W+0.6Cb



946 (VA-81), W+0.6Cb + 0.06Zr



947 (VA-82), W+0.6Cb + 0.04Ti

2800°F for 150 minutes

3200°F for 20 minutes

Figure 34 - Effect of Recrystallization Heat Treatment on W+0.6Cb Extrusion Samples that were Annealed and Reduced 55% by Forging.

Electrolytic Polish - Murakami's Etch - 100X



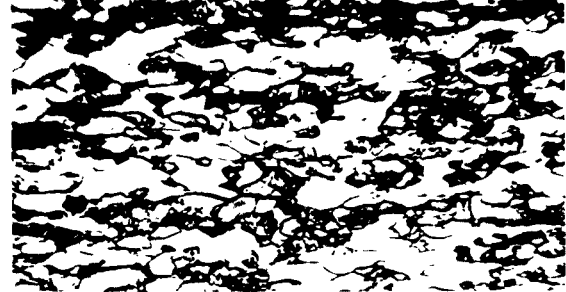
935 (VA-78)



955 (VA-85), 0.12%Zr



936 (VA-79)



956 (VA-86)



946 (VA-81), 0.06%Zr



964 (VA-89), 0.12%Zr + 0.04%Ti



947 (VA-82), 0.04%Ti



965 (VA-90), 500ppm O

Figure 35 - Microstructures of W+0.6Cb Extrusion Samples Reduced 40% by Swaging. Electrode Additions are Indicated.

Electrolytic Polish - Murakami's Etch - 100X



935 (VA-78)



955 (VA-85), 0.12%Zr



936 (VA-79)



956 (VA-86)



946 (VA-81), 0.06%Zr



964 (VA-89), 0.12%Zr + 0.04%Ti



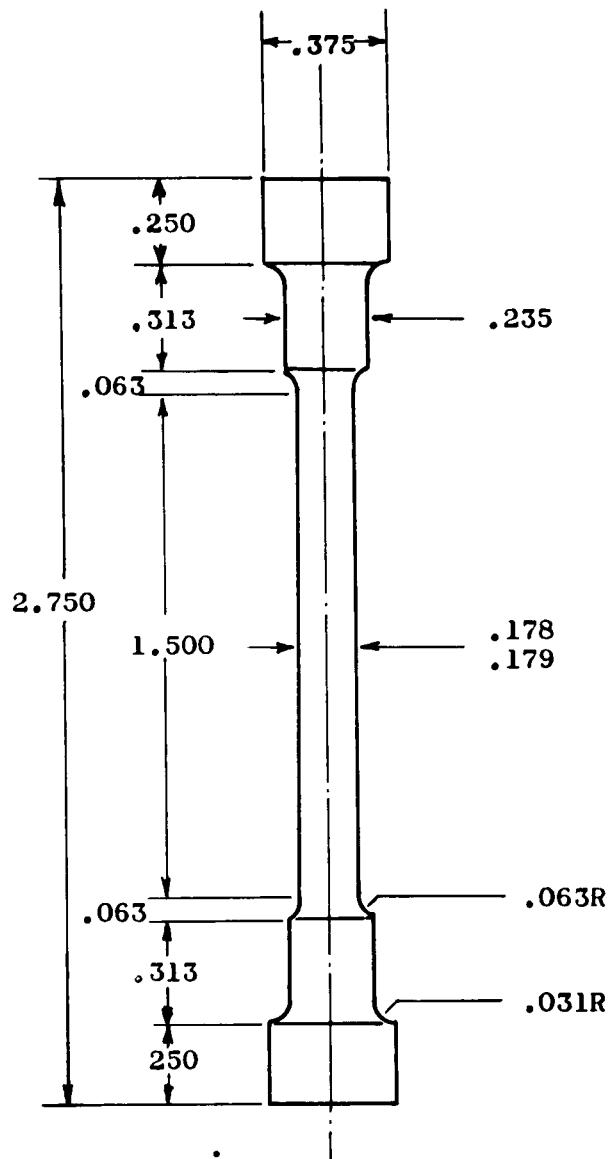
947 (VA-82), 0.04%Ti



965 (VA-90), 500ppm O

Figure 36 - Microstructures of W+0.6Cb Extrusion Samples Reduced 40% by Swaging, Annealed, Reduced Additional 56% by Swaging. Results of Elevated Temperature Testing of These Structures are in Table 12.

Electrolytic Polish - Murakami's Etch - 100X



dimensions are in inches

Figure 37 - Standard Refractory Alloy Vacuum Creep-Rupture Specimen.

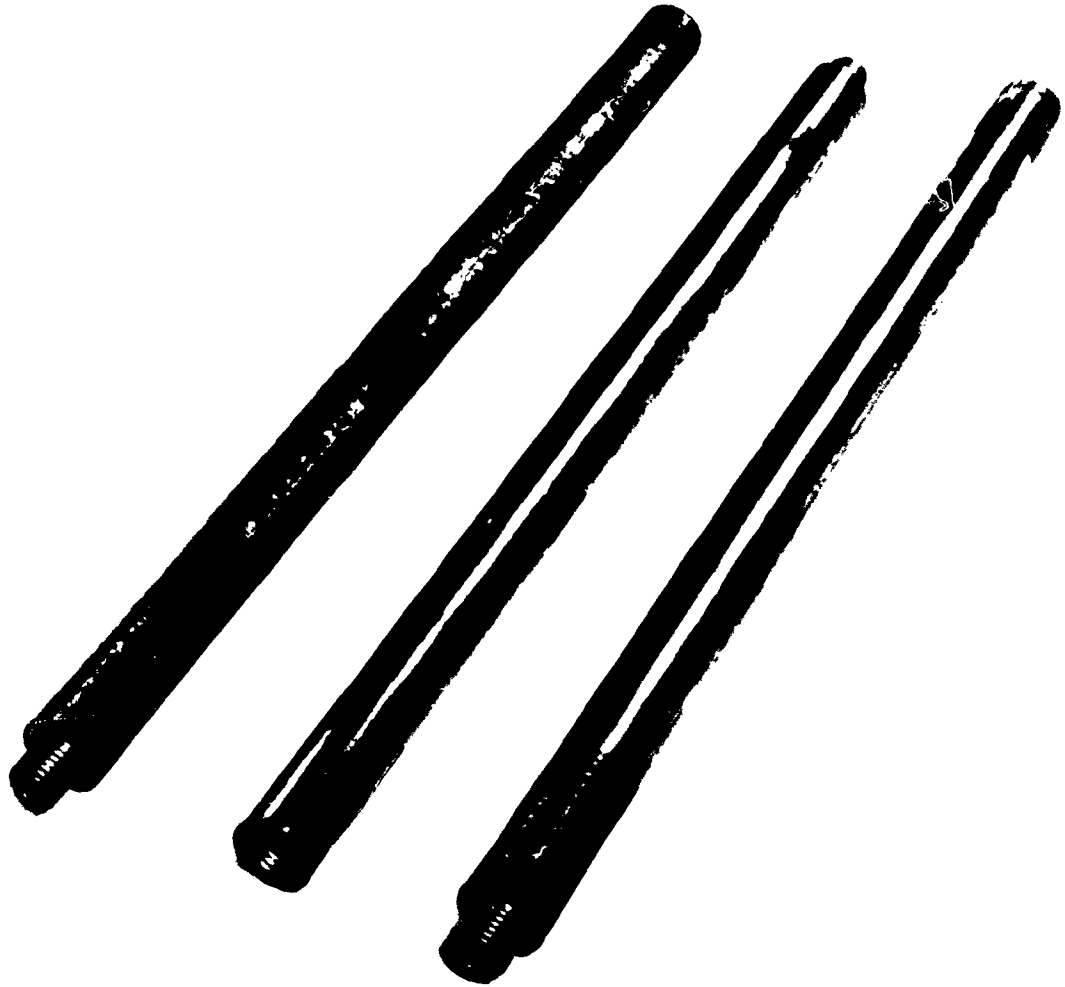


Figure 38 - Threaded Electrode Sections of 94% Tungsten -
6% Molybdenum.

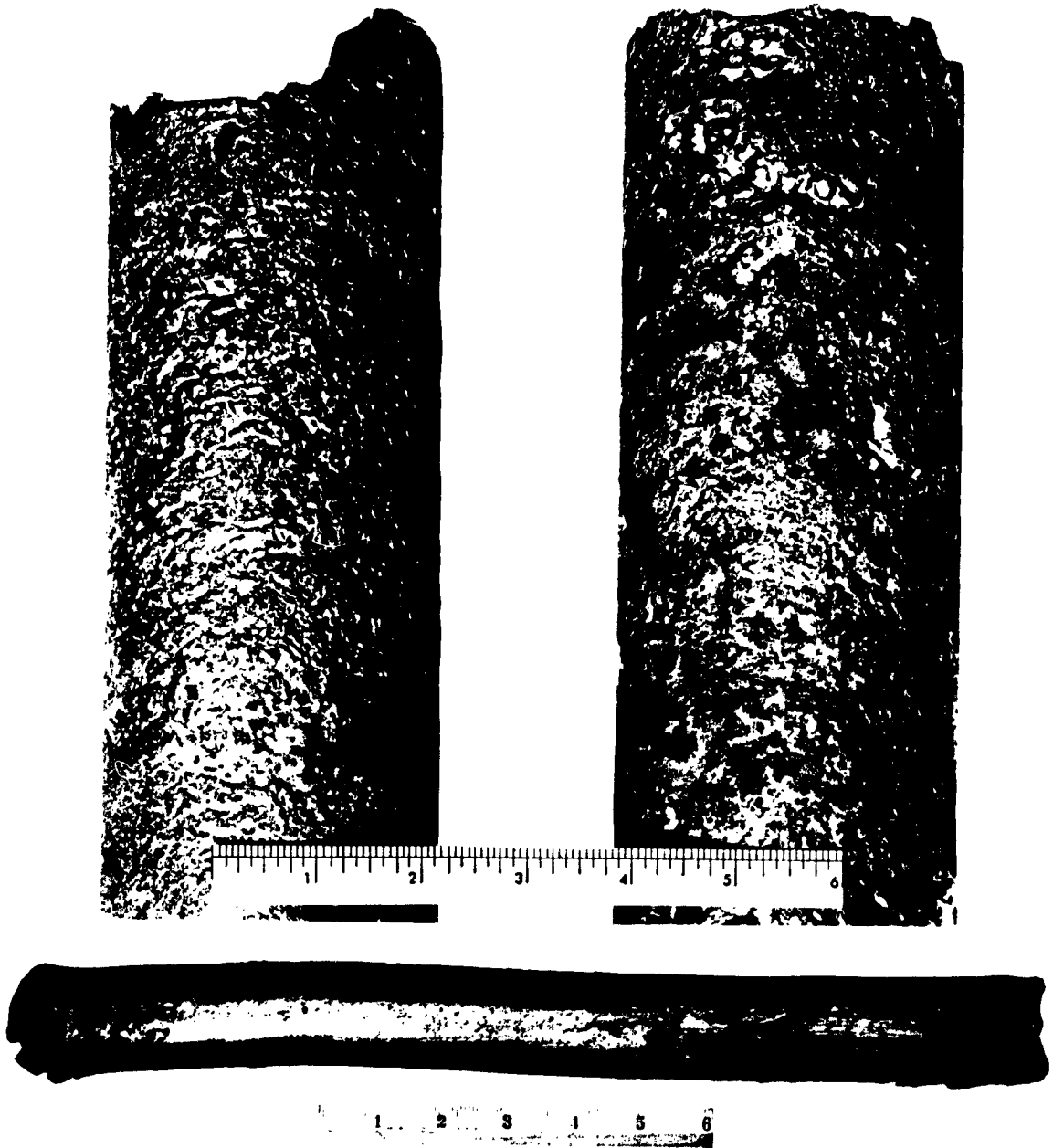


Figure 39 - Ingots of 92-6-2 Alloy Containing Surface Defects. Deep Fissures Are Not Removed By Machining to Billet Diameter and Produce Serious Flaws Shown in Extruded Bar.

MELTING RATE vs. INPUT FOR 92-6-2 ALLOY

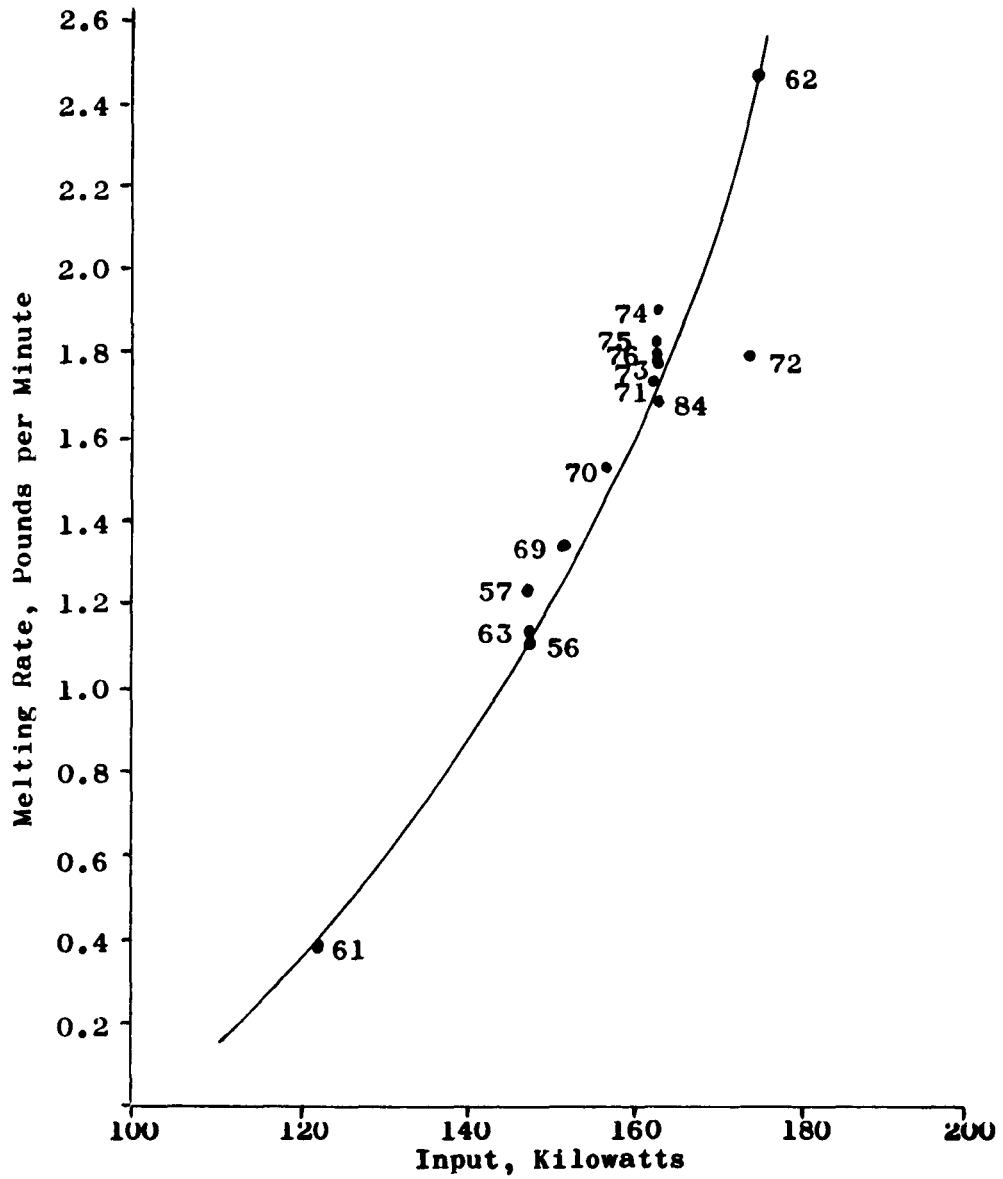
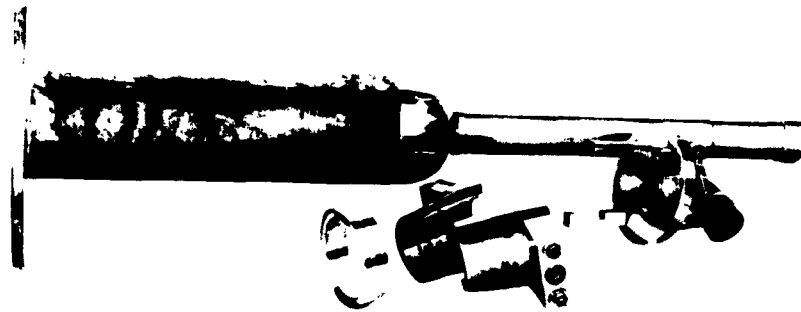


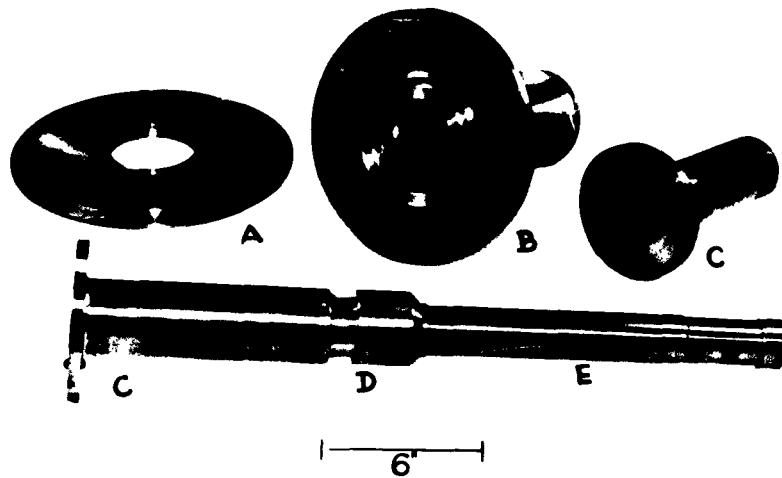
Figure 40



Figure 41 - Ingot of Pure Columbium (VA-77) Produced in 2-Inch Mold. Starting Pad was Composed of Short Lengths of .125"Cb Wire.



3 1/2-Inch Mold with Conductor Tube Attached.
Clamp Ring, Power Connections, and Clamp
Base Are Shown Also.



2-Inch Mold Adapted to Existing Conductor Tube.
Other Items Are: (a) Furnace Adapter Plate,
(b) Jacket Liner, (c) 2-Inch Mold, (d) Mold
Bottom, and (e) Conductor Tube.

Figure 42 - Comparison of 3 1/2-Inch and 2-Inch
Molds and Accessories.

1. Vacuum arc melting
2. Tungsten
3. Columbium
- I. AFSC Project 7351, Task 735101
- II. Contract AF 33 (616)-7459
- III. Westinghouse Electric Corp. Blairsville, Pa.
- IV. G. A. Reimann
- V. Aval fr OTS
- VI. In ASTIA collection

Aeronautical Systems Division, Dir/Materials and Processes, Metals and Ceramics Lab, Wright-Patterson AFB, Ohio.
 Rpt Nr ASD-TDR-63-296. VACUUM ARC MELTING OF TUNGSTEN + 0.6 COLUMBIUM. Final Report, Apr 63, 84p. incl illus., tables, 11 refs.
 Unclassified Report

Vacuum arc melting techniques were developed to produce sound 3/4-inch and 4-inch diameter ingots of tungsten base alloys. The effect of melting rate on ingot characteristics was determined and the effects of carbon, oxygen, zirconium, and titanium on melting characteristics, ingot structure, extrudability, recrystallization, and high temperature tensile properties of the W+0.6Cb alloy were studied also.
 Refinement of ingot structure was produced

1. Vacuum arc melting
2. Tungsten
3. Columbium
- I. AFSC Project 7351, Task 735101
- II. Contract AF 33 (616)-7459
- III. Westinghouse Electric Corp. Blairsville, Pa.
- IV. G. A. Reimann
- V. Aval fr OTS
- VI. In ASTIA collection

Aeronautical Systems Division, Dir/Materials and Processes, Metals and Ceramics Lab, Wright-Patterson AFB, Ohio.
 Rpt Nr ASD-TDR-63-296. VACUUM ARC MELTING OF TUNGSTEN + 0.6 COLUMBIUM. Final Report, Apr 63, 84p. incl illus., tables, 11 refs.
 Unclassified Report

Vacuum arc melting techniques were developed to produce sound 3/4-inch and 4-inch diameter ingots of tungsten base alloys. The effect of melting rate on ingot characteristics was determined and the effects of carbon, oxygen, zirconium, and titanium on melting characteristics, ingot structure, extrudability, recrystallization, and high temperature tensile properties of the W+0.6Cb alloy were studied also.
 Refinement of ingot structure was produced

(over)

(over)

by 0.06 and 0.12% zirconium additions and by increasing the melting rate. Coarsening of ingot structure was produced by 0.04% titanium and 500 to 1000 ppm oxygen additions. W+0.6Cb ingots containing more than 50 ppm carbon could not be extruded, and correlation between extrudability and carbon content below 50 ppm was not found. Adding 0.12% zirconium to the W+0.6Cb alloy significantly improved the 30000F tensile properties.

by 0.06 and 0.12% zirconium additions and by increasing the melting rate. Coarsening of ingot structure was produced by 0.04% titanium and 500 to 1000 ppm oxygen additions. W+0.6Cb ingots containing more than 50 ppm carbon could not be extruded, and correlation between extrudability and carbon content below 50 ppm was not found. Adding 0.12% zirconium to the W+0.6Cb alloy significantly improved the 30000F tensile properties.